



Molecular Fingerprints Are Strong Models for Peptide Function Prediction

Jakub Adamczyk^{id},*,† Piotr Ludynia^{id}† and Wojciech Czech^{id}

Faculty of Computer Science, AGH University of Krakow, al. Mickiewicza 30, 30-059, Krakow, Poland

*Corresponding author, jadamczy@agh.edu.pl

†Those authors contributed equally to this work.

Abstract

Motivation: Understanding peptide properties is often assumed to require modeling long-range molecular interactions, motivating complex graph neural networks and pretrained transformers. Whether such long-range dependencies are essential remains unclear. We investigate if simple, domain-specific molecular fingerprints can capture peptide function without these assumptions. Atomic-level representations aim to provide richer information than purely sequence-based models and better efficiency than structural ones.

Results: Across 132 datasets, including LRGB and five additional peptide benchmarks, models using count-based ECFP, Topological Torsion, and RDKit fingerprints with LightGBM achieve state-of-the-art accuracy. Despite encoding only short-range molecular features, these models outperform GNNs and transformer-based approaches. Control experiments confirm that fingerprints, though inherently local, suffice for robust peptide property prediction. Our results challenge the presumed necessity of long-range interaction modeling and highlight molecular fingerprints as efficient, interpretable, and lightweight alternatives.

Contact: jadamczy@agh.edu.pl

Supplementary information: All code and data are available at:

https://github.com/scikit-fingerprints/peptides_molecular_fingerprints_classification

Key words: peptide function prediction, machine learning, chemoinformatics, molecular fingerprints

Introduction

Peptides are short chains of amino acids, typically composed of 3–50 residues, that perform diverse biological functions and are increasingly being studied as potential therapeutics. They can bind to proteins, regulate their activity, and show antiviral, antitoxin, anticancer, and antidiabetic properties [18, 47]. In particular, antimicrobial peptides (AMPs) are promising candidates against the growing antimicrobial resistance crisis [42]. Therefore, accurate prediction of peptide properties is essential for drug discovery.

Peptide function prediction poses unique challenges for machine learning (ML), including homology bias and imbalanced datasets [12, 40]. Consequently, numerous benchmark datasets with standardized evaluation procedures have been created. Peptides can be represented through various modalities, influencing the choice of ML models. When 3D structures are available, structural encodings can be used [41], but these are rare and computationally expensive to obtain. Thus, sequence- and graph-based representations that avoid folding simulations have gained more attention.

Recent years have seen a shift from handcrafted sequence features to pretrained protein language models (PLMs) such

as ProtBERT and ESM [10, 29]. Alternatively, peptides can be modeled as molecular graphs, enabling the use of Graph Neural Networks (GNNs) and Graph Transformers (GTs). The Long-Range Graph Benchmark (LRGB) [9] formulated peptide prediction as a long-range dependency problem. However, the practical importance of long-range interactions in short and flexible peptides remains unclear.

In chemoinformatics, molecular fingerprints - compact encodings derived from small molecular subgraphs [44] - are widely used for prediction of small-molecule properties. They offer domain-specific, efficient representations that often rival deep learning methods [22, 48]. Despite their success, their use for peptide prediction has been limited, with only a few hybrid approaches that incorporate binary fingerprints [23, 43].

In this work, we revisit count-based molecular fingerprints as features for peptide function prediction. When combined with a LightGBM classifier, these representations achieve state-of-the-art results across six benchmarks, including LRGB, without requiring hyperparameter tuning or 3D structural information. This suggests that short-range subgraph statistics may be sufficient to capture key biochemical features, challenging the assumption that long-range dependencies are essential.

Our contributions are threefold, as we (1) demonstrate that count-based molecular fingerprints outperform alternative models on 132 datasets, (2) provide the most comprehensive benchmark of fingerprint-based peptide models to date, and (3) we analyze the proposed method in controlled experiments, showing its robustness.

Related works

Prediction approaches for peptides differ mainly by representation. For atom-level graphs, message-passing GNNs such as GCN, GraphSAGE, and GIN rely on local neighborhood aggregation [25, 19, 50]. Graph Transformers replace message passing with attention mechanisms, typically with sparsified or semi-local variants, rather than fully global attention, to manage computational cost. Their architectures, like GraphGPS, HDSE, GRIT, GraphViT, and S²GCN, aim to combine local and long-range modeling, and report strong performance on peptides datasets in LRGB benchmark [35, 30, 31, 20, 16].

Sequence-based pipelines remain competitive, especially when data is scarce. They derive physicochemical and compositional descriptors (e.g. amphiphilicity, hydrophobicity) and use classical classifiers like RandomForest or SVM. Notable examples include Ampir, MACREL and amPEPpy [13, 38, 27], and early deep learning models such as AMPScannerV2 [46]. More recently Protein Language Models (PLMs), based on transformer architecture, such as ProtBERT and ProtT5 gained popularity, utilizing pretraining on large protein corpora [10]. The ESM family of models shows a scaling behavior similar to LLMs and give strong results on independent peptide benchmarks [29, 12]. For AMPs, specialized PLMs are available, e.g., BERT-Protein, LMPred, cAMPs-pred, and AMP-BERT [53, 7, 32, 28].

Our work differs in adopting domain-specific, count-based molecular fingerprints as peptide structure encoders. Compared with deep models, they provide robust, low-parameter features and, as we show, give strong performance in peptide function prediction tasks without incorporating long-range mechanisms.

Methods

Here, we describe the molecular fingerprints that form our proposed atom-level peptide encoding. We also describe the approach of Long Range Graph Benchmark to testing the presence of long-range dependencies.

Molecular fingerprints

Molecular fingerprints are feature extraction algorithms for molecules, based on extracting small subgraphs and detecting their presence (binary variant) or counting occurrences (count variant). This turns the problem of molecular graph classification into tabular classification, typically combined with tree-based ensembles such as Random Forest or LightGBM [24]. See Figure 1 for visualization of the proposed pipeline.

We focus on hashed fingerprints [44], exemplified by ECFP [37] or Topological Torsion [33]. They are more flexible than structural fingerprints like MACCS or PubChem, which use predefined subgraphs like functional groups, and are not designed for peptides. Hashed fingerprints use a more flexible approach, defining a general “shape” of extracted subgraphs, for example, circular atom neighborhoods in ECFP [37], paths of given length

in Topological Torsion (TT) [33], or all small subgraphs in RDKit fingerprint [1]. Extracting subgraph features in this manner avoids predefining features explicitly, offering greater flexibility. Subgraphs are defined by their structure, including the specific atoms and bonds they contain (e.g. characterized by atomic numbers and bond types), which are then converted into unique integer identifiers. To obtain a constant-length representation, they are hashed into the output vector, typically using the modulo function. The binary variant only indicates whether a given substructure appears in a molecule at all, while the count-based variant tallies the occurrences, incorporating more information about the compound composition and size.

ECFP typically uses circular subgraphs of radius 2 (see Figure 2). It starts with the atom itself, creating a numerical identifier based on atomic number, number of heavy neighbors, valence, and a few other simple features (see [37] for a complete list). Then, it iteratively increases the radius, incorporating neighbors by combining their identifiers, up to a given maximal radius. This results in the final subgraph identifier for each atom. Such a procedure, known as the Morgan algorithm, closely resembles the operation of message passing in GNNs, as both are rooted in the Weisfeiler-Lehman isomorphism test. Topological Torsion [33], designed to model short-range molecular interactions, encodes linear paths of length 4, combining the identifiers of these consecutive atoms. RDKit fingerprint [1] uses all subgraphs of size up to 7 bonds, which can be nonlinear and include cycles (e.g. rings). The major difference between TT and RDKit is that the former uses only linear paths, while the RDKit fingerprint also encodes small cyclic structures.

The shapes of subgraphs extracted by ECFP with radius 2 are roughly equivalent to those of a shallow 2-layer GNN [8]. However, fingerprints do not learn task-specific weights like GNNs, instead performing domain-specific, deterministic feature extraction. This naturally reduces their risk of overfitting and increases the robustness of the learned feature space [22, 48], particularly beneficial in small, noisy datasets typical in chemo- and bioinformatics.

We focus on the three aforementioned fingerprints, as they are strictly local, very short-range descriptors. Therefore, a good performance of models based on their features can be attributed only to the importance of the short-range relations, rather than to long-range dependencies, since they are inherently incapable of

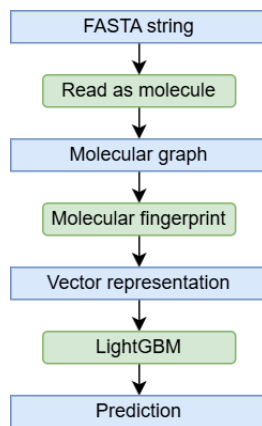


Fig. 1: The proposed pipeline for peptide function prediction.

capturing them. This locality makes them notably fast to compute [3] and scalable to larger molecules like peptides, e.g. ECFP scales linearly with the number of atoms. Because peptides are relatively linear structures, path-based TT and RDKit fingerprints also scale well. Those three fingerprints have also shown remarkable performance in ligand-based virtual screening [36].

Lastly, we note that molecular fingerprints do not require any information about molecular conformation, peptide folding, or even whether a stable structure exists at all. Atom-level graphs (see Figure 3 for an example) can be quickly and deterministically constructed from an amino acid sequence, and then vectorized by a fingerprint algorithm.

Long-range interactions (LRI)

Long Range Graph Benchmark (LRGB) [9] proposed 3 conditions for a dataset to potentially require learning long-range interactions (LRI). Firstly, a necessary condition is that the graphs must be sufficiently large, significantly exceeding the typical GNN receptive field. Secondly, the nature of the task itself must require long-range dependencies between nodes, with local interactions being insufficient. Lastly, the experiments should confirm this - models with global knowledge, such as GNNs with topological encodings or graph transformers, must outperform local message-passing ones. For graph classification and regression, peptide property prediction was proposed as a task family meeting these conditions.

We show that this is not necessarily the case, especially for the third condition. While atomic-level peptide graphs are large and elongated (large diameter, low atom degrees) enough to suggest potential LRI, the biological motivation for such interactions in peptide property prediction is weaker than for larger proteins. In

proteins, LRI arise from complex folding driven by distant amino acid interactions and strongly influence functional properties. By contrast, the smaller size of peptides naturally limits these effects and often leads to a lack of well-defined structure [21].

The third point, namely the superior performance of models with global knowledge, is the easiest to validate quantitatively. Since the argument is based on experimental results, it suffices to show that inherently local short-range models outperform long-range ones. Molecular fingerprints exactly fulfill these requirements. By obtaining SOTA results, we show that they provide strong evidence against the third claim, indicating that peptide function prediction primarily depends on short-range interactions.

Experiments and results

We train the proposed fingerprint-based models on a diverse set of benchmarks covering a wide range of peptide properties, data sampling strategies, evaluation metrics, and train-test splits. We closely follow the procedures of the original benchmark publications and report the corresponding metrics. When multiple metrics are available, we report AUROC and Matthews Correlation Coefficient (MCC) due to space constraints, with the remaining metrics provided in the Supplementary Material. The best result in each table is highlighted in bold.

Our proposed fingerprint-based models use count variants throughout and are implemented with the `scikit-fingerprints` [3] library. We use default values for all hyperparameters: ECFP radius 2 (diameter 4, i.e., ECFP4), Topological Torsion path length 4, and RDKit fingerprint path length 7. They use small subgraphs as features, capturing only very short-range dependencies. We observed no significant performance gains from hyperparameter tuning (except for PeptideReactor, see Section 4.3).

We use LightGBM [24] with 500 trees as the classifier due to its robust performance. Since most datasets are highly imbalanced, we apply class weighting inversely proportional to the positive class frequency. All other hyperparameters are kept at their default values, as tuning yielded negligible improvements. Increasing the number of trees beyond the default 100 was the only change that consistently improved performance, in line with prior literature [34].

The proposed method’s low sensitivity to hyperparameters is advantageous, as it reduces computational cost for new tasks, especially in large-scale virtual screening of peptide therapeutics. It also provides a fast and easy-to-use baseline for future works in this area.

Long Range Graph Benchmark (LRGB)

We first report results on the LRGB [9] benchmark for both datasets - *Peptides-func* (classification) and *Peptides-struct* (regression) - in Table 1. These are multioutput datasets, and we report metrics averaged across all tasks. We compare against a broad set of graph-based architectures, including the original Graph Transformer and SAN [9], as well as more recent models such as the MOLTOP baseline [2], well-tuned classical GNNs (GCN, GatedGCN, GINE) [45], and models with enhanced long-range capabilities including GRIT [31], HDSE [30], and S²GCN [16].

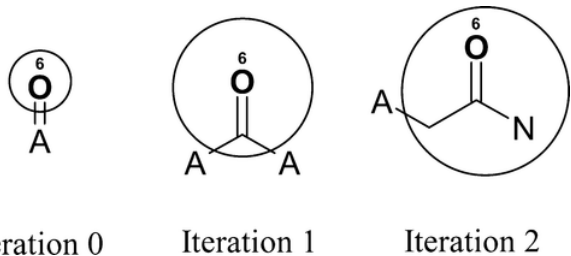


Fig. 2: Example subgraph extraction in consecutive iterations of ECFP algorithm. Reprinted with permission from [37]. Copyright 2010 American Chemical Society.

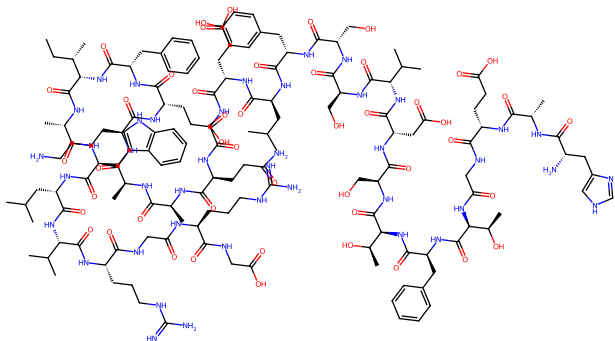


Fig. 3: Atom-level molecular graph for Liraglutide peptide.

Table 1. The results on LRGB benchmark.

Model	Peptides-func AUPRC \uparrow	Peptides-struct MAE \downarrow
Transformer	63.26 \pm 1.26	0.2529 \pm 0.0016
SAN	64.39 \pm 0.75	0.2545 \pm 0.0012
MOLTOP	64.59 \pm 0.05	-
GraphGPS	65.35 \pm 0.41	0.2500 \pm 0.0005
GINE	66.21 \pm 0.67	0.2473 \pm 0.0017
GatedGCN	67.65 \pm 0.47	0.2477 \pm 0.0009
GCN	68.60 \pm 0.50	0.2460 \pm 0.0007
GraphViT	69.42 \pm 0.75	0.2449 \pm 0.0016
GRIT	69.88 \pm 0.82	0.2460 \pm 0.0012
CRaWl	70.74 \pm 0.32	0.2506 \pm 0.0022
GRED	71.33 \pm 0.11	0.2455 \pm 0.0013
DRew	71.50 \pm 0.44	0.2536 \pm 0.0015
HDSE	71.56 \pm 0.58	0.2457 \pm 0.0013
S ² GCN	73.11 \pm 0.66	0.2447 \pm 0.0032
RDKit	73.11	0.2459
TT	73.18	0.2438
ECFP	74.60	0.2432

Table 2. Differences between binary and count fingerprint models.

Dataset	Variant	ECFP	TT	RDKit
Peptides-func	binary	70.57	66.18	63.88
Peptides-func	binary + length	68.46	66.49	66.97
Peptides-func	count	74.60	73.18	73.11
AUPRC gain \uparrow		+4.03	+7.00	+9.23
Peptides-struct	binary	0.3049	0.3298	0.3331
Peptides-struct	binary + length	0.2652	0.2691	0.2744
Peptides-struct	count	0.2432	0.2438	0.2459
MAE gain \downarrow		-0.0617	-0.0860	-0.0872

Since both datasets are multitask and LightGBM supports only single outputs, we train a separate model per task. For *Peptides-struct*, we optimize MAE loss function. LRGB results for GNNs are reported over 10 random seeds. LightGBM with default settings is deterministic, so we do not report standard deviations. Results for Random Forest and Extremely Randomized Trees, which depend on random seed, are provided in the Supplementary Material. Their standard deviations are very low, < 0.1 AUPRC.

The key observation is that all fingerprint-based models achieve SOTA results on both datasets. The strictly local ECFP model, based on radius 2 subgraphs, exceeds the best long-range GNN, S²GCN, by 1.5% AUPRC. Topological Torsion and RDKit fingerprint obtain similar results. The fact that these inherently short-range models reach such a performance contradicts the conclusions of [9] that incorporating long-range dependencies is necessary for accurate peptide function prediction. Instead, our results underscore the dominant role of short-range interactions.

The ECFP4 fingerprint functions similarly to a two-layer message-passing GNN, yet it outperforms both local models (e.g., GCN) and long-range variants such as S²GCN and HDSE. We attribute this to three factors.

First, fingerprints count discrete substructures rather than learning continuous graph representations. This provides a stronger inductive bias and reduces reliance on large training datasets.

Second, peptides consist of repeating fragments, amino acids, that are structurally similar and recur frequently. Thus, models mainly need to detect recurring small subgraphs (e.g., amine groups, -NH₂). This is not indicative of genuine long-range interaction, but rather reflects the straightforward repetition of common motifs across different regions of the input.

Third, count-based fingerprints naturally capture effects of structure size and substructure frequency. In *Peptides-struct*, regression targets such as inertia mass and length strongly correlate with peptide size. In *Peptides-func*, classification labels (e.g., antimicrobial activity) depend on binding properties linked to surface area and thus size. These properties are therefore more closely tied to local structures and overall peptide size than to long-range interactions, and can be well approximated by counting subgraphs.

Our results therefore indicate that the *Peptides-func* and *Peptides-struct* datasets do not require modeling long-range interactions. Previous studies may have overlooked this, as [9] evaluated only GNNs, and [45] focused on deep models (6 to 10 layers) with global topological encodings. This underscores the importance of comparing against established, domain-specific baselines for a fair evaluation. To emphasize the effect of count-based fingerprints, we compare them with (1) binary variants (2) binary variants with sequence length feature, see Table 2. We observe substantial performance gains from using count features instead of binary ones. They also strongly outperform binary fingerprints with sequence length, meaning that the count-based model does not simply approximate the overall peptide size. Given those findings, it is concerning that all hybrid models in the bioinformatics literature we reviewed [23, 43] rely exclusively on binary fingerprints, despite count variants having identical computational cost and markedly better performance.

We also highlight the efficiency of our approach. In terms of wall-clock time, computing ECFP fingerprints and training LightGBM takes 19 seconds on a 12-core Intel Core i7-12700KF CPU for *Peptides-func*. In contrast, training the SAN graph transformer requires up to 60 hours on an NVIDIA A100 GPU [9]. Additional timing results are provided in the Supplementary Material.

Antimicrobial peptides (AMPs) benchmarks

In subsequent experiments, we examine whether the LRGB results generalize to other benchmarks in this domain. Such generalization would indicate that peptide function prediction is not inherently dependent on long-range interactions.

We first report results on antimicrobial peptide (AMP) prediction benchmarks. Although those benchmarks target the same property, antimicrobial activity, they differ in structural diversity, construction of positive and negative examples, and train-test splitting procedures. We consider three benchmarks that span these variations: the BERT-based models benchmark [15], XUAMP [49], and AMPBenchmark [40]. Notably, many datasets in this section include peptides that exceed the typical length definition, with averages of 70-100 amino acids. Achieving strong performance therefore requires fingerprint-based models to be both scalable, due to atom-level processing, and effective on substantially larger molecules. We include detailed dataset descriptions and sequence length statistics in Supplementary Material.

Table 3. The results on BERT-based models benchmark [15].

Model	ADAPTABLE	APD	CAMP	dbAMP	DRAMP	YADAMP	Average F1
AMP-BERT	81.7	78.3	82.3	62.7	64.0	82.6	75.3
BERT-Protein	79.4	90.1	80.6	82.9	58.8	58.8	75.1
cAMPs_pred	61.3	74.1	72.8	52.4	39.2	85.0	64.1
LM_pred	55.9	71.7	64.5	60.7	47.6	82.1	63.8
LM_pred (BFD)	73.9	89.6	83.6	68.7	64.8	84.4	70.3
RDKit	82.0	93.0	88.4	91.4	76.4	92.0	87.2
TT	80.6	94.3	88.8	90.8	76.9	95.8	87.8
ECFP	80.8	93.0	88.2	91.5	76.3	95.8	87.6

BERT-based models benchmark

First, we compare our approach with BERT-based models pretrained for AMP prediction, as evaluated in [15]. This benchmark includes AMPs from six classic datasets, uses negative samples from UniProt, and applies CD-HIT [14] with a 40% similarity threshold to reduce homology bias. No additional fine-tuning is performed, as the BERT models are already trained specifically for AMP prediction, including classification heads. The authors also note that parts of these datasets may be present in the pretraining data, which likely benefits the BERT models on this benchmark. To mimic such pretraining with fingerprints and LightGBM, we adopt a leave-one-dataset-out strategy. For example, when evaluating on the ADAPTABLE dataset, we merge all remaining datasets into a single training set and apply CD-HIT-2D [14] at a 40% threshold to remove peptides overly similar to those in the test set.

Results are reported in Table 3, focusing on F1 score, as all models achieve nearly identical AUROC values close to 100%. Additional metrics are provided in the Supplementary Material. Fingerprint-based models achieve state-of-the-art performance on all datasets, with Topological Torsion (TT) yielding the best average F1 score. Performance differences vary by dataset but show no clear dependence on test set size or peptide size. For instance, ADAPTABLE and DRAMP both contain approximately 4000 peptides with an average length of 75 amino acids, yet differ substantially in difficulty. On ADAPTABLE, fingerprints improve F1 by 0.3% over the best BERT-based model, while on DRAMP the gain reaches 12.1%. These results demonstrate that atom-level, short-range fingerprints consistently yield strong models, but the exact data used for training has a considerable impact on the final performance.

XUAMP benchmark

Datasets used in the previous section are widely adopted in AMP research, but are relatively small. To address this limitation, a unified AMP benchmarking dataset known as XUAMP was proposed [49]. It is constructed from nine commonly used datasets, such as CAMP and DRAMP, which are merged and deduplicated using homology-based CD-HIT clustering [14]. This prevents data leakage by ensuring that highly similar sequences do not appear in both training and test sets, ensuring a realistic evaluation. The authors benchmarked traditional feature engineering approaches combined with various classifiers, including Random Forest, SVM, and k nearest neighbors (kNN).

We exactly replicate the original XUAMP setup and data splits, and report the results in Table 4. Fingerprint-based models again achieve SOTA performance, demonstrating robustness across different dataset sizes. The strongest prior method, AMPfun

Table 4. The results on XUAMP benchmark [49].

Method	AUROC	MCC
AMPscannerV2	58.5	0.137
iAMP-2L	59.2	0.261
ADAM-SVM	61.2	0.264
ampir	61.9	0.156
MLAMP	62.9	0.194
ADAM-HMM	68.4	0.39
AMPlify	69.7	0.381
AMPEP	72.7	0.425
AMPfun	73.5	0.414
RDKit	74.5	0.404
TT	73.1	0.385
ECFP	75.0	0.429

[6], relies on a relatively complex pipeline that combines binary amino acid position profiles, sequence composition features, physicochemical descriptors, and feature selection. Such pipelines can be fragile, as evidenced by the superior performance of the much simpler ECFP fingerprint in both AUROC and MCC.

AMPBenchmark

The authors of AMPBenchmark [40] observed that negative class sampling has a strong impact on model performance. Their benchmark evaluates the sensitivity of AMP predictors to data choice by retraining models across a large collection of datasets with varying negative sampling strategies. Evaluated models range from sequence-based feature engineering approaches, such as AmpGram [4], through CNN-based deep learning models like Deep-AmPEP30 [51], to multimodal ensembles combining physicochemical and sequence features, such as ampir [13].

Model robustness is assessed by retraining on a suite of datasets constructed by pairing the same positive class peptides with 11 different negative sampling strategies, each repeated five times using distinct UniProt subsets. This yields 55 datasets that vary in sequence length distributions, sequence similarity, and class balance, each evaluated using an 80-20% train-test split. Results on AMPBenchmark are summarized in Table 5, reporting the mean and standard deviation across all retraining runs. Once again, fingerprint-based models achieve the best performance, with substantially lower standard deviations than competing methods. This suggests that feature engineering based on peptide topological graph yields more robust and reliable models than complex ensembles. Despite their popularity in bioinformatics, the latter are inherently susceptible to data sampling strategy and human bias in descriptor selection.

Table 5. The results on AMPBenchmark [40].

Model	AUROC
AmPEP	61.69 \pm 6.93
iAMP-2L	62.60 \pm 9.51
SVM-LZ	79.71 \pm 2.43
CS-AMPPred	86.69 \pm 4.36
AMAP	89.87 \pm 4.18
Deep-AmPEP30	90.98 \pm 5.61
AmPEPpy	95.35 \pm 2.99
AmpGram	95.56 \pm 2.54
MACREL	96.29 \pm 2.43
MLAMP	96.68 \pm 2.35
ampir	96.71 \pm 2.08
AMPScannerV2	96.79 \pm 2.08
TT	97.19 \pm 1.89
RDKit	97.25 \pm 1.84
ECFP	97.37 \pm 1.74

General peptide benchmarks

Beyond antimicrobial activity, many other peptide properties are of interest, including antioxidant activity, anti-MRSA effects, toxicity, and more. A common challenge in this area is the small size of available datasets, which often contain fewer than 1000 positive samples. To assess how fingerprint-based models perform under these constraints, we selected two large benchmarks comprising a total of 68 datasets that span a wide range of peptide properties: AutoPeptideML [12] and PeptideReactor [41].

AutoPeptideML

AutoPeptideML [12] comprises 18 datasets. Positive peptides are drawn from existing literature datasets, while negative ones are carefully filtered to avoid false negatives and sampled to match the sequence length distribution of the positives. Train-test splits are created using homology clustering to produce an out-of-distribution test set, analogous to scaffold splits commonly used in molecular property prediction. Together, these choices result in a particularly challenging evaluation setup. AutoPeptideML reports results for state-of-the-art protein language models (PLMs), including models with up to 3B parameters, such as Prot-T5-XL [10]. Their embeddings are combined with a complex ensemble of 30 classifiers: 10 k nearest neighbors (kNN), 10 Random Forests, and 10 LightGBMs, each tuned separately via Bayesian hyperparameter optimization.

Results are summarized in Table 6. Fingerprint-based models are competitive in both MCC and AUROC with the best performing PLMs. Importantly, they are far more parameter-efficient, reaching comparable performance with roughly 22k parameters (counting tree nodes in LightGBM), compared to PLMs with up to 3 billion weights. Notably, the ECFP-based classifier outperforms three variants of ESM2 [29] in both AUROC and MCC, and achieves MCC nearly identical to ESM2-650M. A likely explanation is that peptides, unlike most proteins used to train and evaluate PLMs, are very short sequences. Fingerprints operate on full molecular graphs and can be viewed as a higher-resolution representation of peptides than sequence-only models.

Table 6. The results on AutoPeptideML benchmark [12].

Model	# params	AUROC	MCC
ProtBERT	420M	75.9	0.375
ESM2-150M	150M	77.7	0.402
Prot-T5	3B	77.1	0.409
ESM2-8M	8M	77.5	0.418
ESM2-35M	35M	78.0	0.428
ESM1b-650M	650M	78.9	0.433
ESM2-650M	650M	79.7	0.438
Prot-T5-XL	3B	79.7	0.447
RDKit	20k	76.9	0.421
TT	23k	77.1	0.422
ECFP	22k	78.1	0.437

PeptideReactor

PeptideReactor [41] is a large benchmark comprising 50 datasets designed to compare peptide encoding methods. To focus on the impact of feature engineering, all models use the same Random Forest classifier with 100 trees. No classifier hyperparameter tuning or class weighting is applied, and only the feature extraction methods are tuned. The benchmark includes 48 encodings based on sequence information or structural descriptors derived from 3D structures. This setting enables a direct comparison of molecular fingerprints with a broad range of established peptide encodings from the bioinformatics literature.

For this benchmark, we perform some limited hyperparameter tuning for fingerprints. We make this exception, since authors explicitly encourage tuning for feature extraction, and perform it for many other methods, so tuning fingerprints results in more fair comparison. Further, many datasets in this benchmark contain relatively large proteins, which may benefit from slightly larger subgraphs in fingerprints. Specifically, 17 of the 50 datasets have average sequence lengths exceeding 50 amino acids, the typical upper limit for peptides, and 8 exceed 200 amino acids. See Supplementary Material for detailed statistics of all datasets. Using 5-fold cross-validation, we tune the ECFP radius in the range [2, 4], the Topological Torsion path length in the range [4, 6], and the RDKit path length in the range [7, 9]. These remain short-range descriptors, but allow slightly larger substructures to be captured.

Since this is an encoding benchmark, we also evaluate a general “FP encoding” setting, where the fingerprint type itself is treated as a hyperparameter. This allows us to address the question “How effective are encodings based on the topological graph (2D structure) of a molecule?”. Such comparison is relevant because existing feature groups rely either on amino acid sequences (1D encodings) or spatial peptide structures (3D encodings). It is also a highly realistic setting, as the best encoding method is selected for each dataset. Results are summarized in Table 7. Due to space constraints, we report only the five best sequence- and structure-based encodings here, with full results provided in the Supplementary Material.

Fingerprints significantly outperform all structure-based encodings that rely on spatial information, despite modeling only topological molecular graphs and short-range interactions. This suggests that these smaller proteins may exhibit biological behavior that differs from that of large proteins, for which spatial folding is known to be critical. Moreover, constructing molecular graphs takes only a few seconds, whereas spatial encodings require

Table 7. The results on PeptideReactor benchmark [41].

Model group	Model	Average F1
Structure	disord	53.5
	electr	60.9
	distan	61.3
	delaun	69.5
	qsar	72.8
Sequence	dde	81.3
	ngram_	81.6
	psekraac	81.8
	dist_f	82.2
	cksaap	82.4
Fingerprint	RDKit	80.6
	TT	80.6
	ECFP	81.7
	FP encoding	82.9

costly tertiary structure estimation, taking approximately 85 minutes per dataset [41].

Fingerprints are also highly competitive with the strongest sequence-based methods. Notably, the ECFP fingerprint alone ranks fourth overall in the benchmark, outperforming 45 other encodings. We also observe substantial variation in fingerprint performance across datasets. When treating the fingerprint type as a hyperparameter, the FP encoding achieves state-of-the-art performance. This indicates that fingerprints provide robust peptide representations that scale well across diverse properties and protein sizes, but the optimal choice depends on the data and task. We note that [41] concludes that structural encodings are inferior to sequence-based ones in both computational cost and performance. Fingerprint-based encodings offer a counterexample to this conclusion, albeit relying on a topological 2D structure rather than conformational (spatial) information.

Additional baselines

Two commonly used sequence-based baselines for proteins and peptides are amino acid counts and ESM2 [29]. The former uses a bag-of-words on sequences, typically including uni- and bigram counts. ESM2 embeds a peptide by extracting amino acid embeddings and combining them with mean pooling.

Note that molecular fingerprints can be viewed as a higher-resolution alternative to those methods. They operate directly on atomic graph, rather than on sequences, which enriches the data representation, particularly in realistic low-data regimes. This structural encoding incorporates information about amino acids, such as their elemental composition and charge, capturing structural similarities between amino acids. For example, they encode the fact that asparagine and glutamine are more similar to each other than asparagine and proline. In contrast, sequence-level models must learn these relationships implicitly, often requiring more data.

We compare the two baselines to ECFP fingerprints, with results shown in Table 8. LightGBM classifier is used in all cases except PeptideReactor, where we apply Random Forest as before. We follow the same data splits and evaluation metrics as in the earlier sections. We use the ESM2-35M variant, as larger models did not improve performance, consistent with prior findings [12].

Table 8. Results of additional baselines.

Benchmark	Metric	Amino acid counts	ESM2	ECFP
AMPBenchmark	AUROC	96.9%	97.3%	97.4%
AutoPeptideML	AUROC	74.6%	77.2%	78.1%
BERT benchmark	F1	87.5%	89.8%	87.6%
LRGB, Peptides-func	AUPRC	69.8%	66.0%	74.6%
LRGB, Peptides-struct	MAE	0.2665	0.2828	0.2432
PeptideReactor	F1	80.0%	76.8%	81.7%
XUAMP	AUROC	74.2%	76.8%	75.0%

Molecular fingerprints give the best results in 5 out of 7 cases. They are particularly strong on PeptideReactor, with 4.9% F1-score gain over ESM2. Further, they are always better than amino acid counts, and as such form a strong baseline for peptide property prediction.

Sequence shuffling

To verify that short-range dependencies are sufficient, we conduct sequence shuffling experiments. A given percentage of amino acids in each training sequence is randomly permuted, acting as an adversarial perturbation. As this shuffling ratio increases, long-range interactions are progressively destroyed. If performance remains high even with fully randomized sequences, this indicates that peptide properties mainly depend on substructural composition. Additional experiments (shuffling performance for baselines, shuffling the test sequences) and detailed tables are reported in the Supplementary Material.

We use the ECFP fingerprint with default hyperparameters and report the average metric across each benchmark¹ for every shuffling ratio in Figure 4. Performance degradation for fingerprint-based models is small, even with fully randomized sequences, and does not exceed about 4%. On XUAMP, results are nearly identical to those obtained without shuffling. Thus, even when sequences are completely randomized and only very short-range interactions remain, the ECFP fingerprint maintains strong performance. This further supports the hypothesis that peptide property prediction primarily depends on local, atom-level subgraphs and also demonstrates the robustness of the proposed approach.

Additional experiments

Due to word limitations, we relegate a series of additional experiments to the Supplementary Materials. They further explore the robustness and possible limitations of the proposed approach. Here, we provide summary results.

First, we analyze error distributions and correlate them to physicochemical properties of peptides, but results do not indicate any particular patterns. Further, we explore binning data by length, e.g., testing only on shortest or longest peptides. All models show similar performance patterns, e.g., fingerprints and ESM2 underperform on shortest peptides, which have the least structural information.

Lastly, we purposefully design a long-range task, in order to delineate the limitations of the proposed method. The task is recognizing highly charged sequence motifs like “KKK” or

¹ We exclude AMPBenchmark due to its very large size.

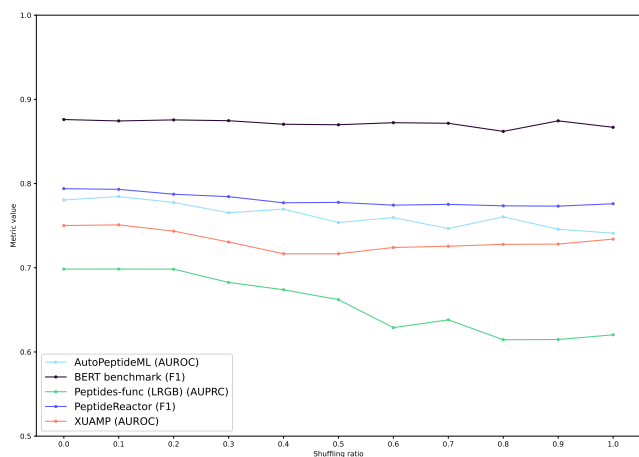


Fig. 4: ECFP performance under increasing shuffling ratio.

“RRR” in sequence, which are known to impact peptide-protein binding and are highly relevant to peptide therapeutic design. It is trivial for sequence-based models like ESM2, which achieve near-perfect performance. However, it is very challenging for molecular fingerprints, as it requires using long-range and order-dependent on molecular graphs.

Conclusions

We presented an approach to peptide function prediction based on count variants of hashed molecular fingerprints. These methods use atom-level representations derived from molecular graphs, which are inexpensive to construct, fast to compute, and do not require knowledge of the folded peptide structure. Despite relying strictly on local, short-range descriptors, they achieve strong performance across a broad range of tasks.

When combined with LightGBM, this approach delivers superior results in a large-scale evaluation spanning six benchmarks and 132 datasets. They outperform a wide range of alternatives, including GNNs, pretrained amino acid sequence transformers, hand-crafted feature engineering pipelines, and multimodal models. Beyond predictive quality, the proposed models are computationally lightweight.

To the best of our knowledge, this work provides the most extensive comparison of molecular fingerprints applied to peptides to date. In contrast to prior bioinformatics studies, we focus on count-based rather than binary fingerprints and show that this design choice is critical for strong performance. Our main methodological contribution is demonstrating that inherently short-range models achieve state-of-the-art results on peptide property prediction tasks. In particular, an ECFP-based classifier with radius 2 surpasses the previous best model on *Peptides-func* dataset from LRGB benchmark by 1.5% AUPRC. These findings challenge the presumed necessity of long-range dependencies for this task and reinforce previous observations in the literature [45].

Future work will extend this approach to property prediction for larger proteins. We also plan to analyze fingerprint performance on tasks involving chemically modified peptides, such as cyclic peptides, which are of high interest for drug design and require atom-level featurization.

In conclusion, atom-level, short-range models based on molecular fingerprints constitute strong and reliable approaches for peptide property prediction. Their use is also essential for critically evaluating claims about the importance of long-range dependencies in molecular learning tasks.

Acknowledgements

The authors thank the BIT Student Scientific Group for computational resources and assistance for this project. The authors thank Aleksandra Elbakyan for her work and support for accessibility of science.

Data availability

All datasets and benchmarks used are publicly available at https://github.com/scikit-fingerprints/peptides_molecular_fingerprints_classification.

Author contributions statement

Contributions follow the CRediT format. J.A. was responsible for conceptualization, methodology, software, validation, investigation, data curation, and writing. P.L. was responsible for software, investigation, and writing. W.C. was responsible for writing, review, and supervision.

Competing interests

No competing interest is declared.

Funding

This work was supported by the general funding from the Ministry of Science and Higher Education to AGH University in Krakow, and by project Excellence Initiative – Research University (IDUB) for AGH University of Krakow.

References

1. The RDKit Book: RDKit Fingerprints. https://www.rdkit.org/docs/RDKit_Book.html#rdkit-fingerprints. Accessed: 2025-01-24.
2. Jakub Adamczyk and Wojciech Czech. Molecular Topological Profile (MOLTOP)-Simple and Strong Baseline for Molecular Graph Classification. In *ECAI 2024*, pages 1575–1582. IOS Press, 2024.
3. Jakub Adamczyk and Piotr Ludynia. Scikit-fingerprints: Easy and efficient computation of molecular fingerprints in Python. *SoftwareX*, 28:101944, 2024.
4. Michał Burdukiewicz, Katarzyna Sidorczuk, Dominik Rafacz, Filip Pietluch, Jarosław Chilimoniuk, Stefan Rödiger, and Przemysław Gagat. Proteomic Screening for Prediction and Design of Antimicrobial Peptides with AmpGram. *International Journal of Molecular Sciences*, 21(12), 2020.
5. Davide Chicco and Giuseppe Jurman. The advantages of the matthews correlation coefficient (mcc) over f1 score and accuracy in binary classification evaluation. *BMC genomics*, 21(1):6, 2020.
6. Chia-Ru Chung, Ting-Rung Kuo, Li-Ching Wu, Tzong-Yi Lee, and Jorng-Tzong Horng. Characterization and identification

- of antimicrobial peptides with different functional activities. *Briefings in Bioinformatics*, 21(3):1098–1114, 06 2019.
7. William Dee. LMPred: Predicting antimicrobial peptides using pre-trained language models and deep learning. *Bioinformatics Advances*, 2(1):vbac021, 2022.
 8. David K Duvenaud, Dougal Maclaurin, Jorge Iparraguirre, Rafael Bombarell, Timothy Hirzel, Alán Aspuru-Guzik, and Ryan P Adams. Convolutional networks on graphs for learning molecular fingerprints. *Advances in Neural Information Processing Systems*, 28, 2015.
 9. Vijay Prakash Dwivedi, Ladislav Rampásek, Michael Galkin, Ali Parviz, Guy Wolf, Anh Tuan Luu, and Dominique Beaini. Long Range Graph Benchmark. *Advances in Neural Information Processing Systems*, 35:22326–22340, 2022.
 10. Ahmed Elnaggar, Michael Heinzinger, Christian Dallago, Ghalia Rehawi, Yu Wang, Llion Jones, Tom Gibbs, Tamas Feher, Christoph Angerer, Martin Steinegger, et al. ProtTrans: Toward Understanding the Language of Life Through Self-Supervised Learning. *IEEE Transactions on Pattern Analysis & Machine Intelligence*, 44(10):7112–7127, 2021.
 11. Thomas W Epps and Kenneth J Singleton. An omnibus test for the two-sample problem using the empirical characteristic function. *Journal of Statistical Computation and Simulation*, 26(3-4):177–203, 1986.
 12. Raúl Fernández-Díaz, Rodrigo Cossio-Pérez, Clement Agoni, Hoang Thanh Lam, Vanessa Lopez, and Denis C Shields. AutoPeptideML: a study on how to build more trustworthy peptide bioactivity predictors. *Bioinformatics*, 40(9):btae555, 09 2024.
 13. Legana C H W Fingerhut, David J Miller, Jan M Strugnell, Norelle L Daly, and Ira R Cooke. ampir: an R package for fast genome-wide prediction of antimicrobial peptides. *Bioinformatics*, 36(21):5262–5263, 07 2020.
 14. Limin Fu, Beifang Niu, Zhengwei Zhu, Sitao Wu, and Weizhong Li. CD-HIT: accelerated for clustering the next-generation sequencing data. *Bioinformatics*, 28(23):3150–3152, 10 2012.
 15. Wanling Gao, Jun Zhao, Jianfeng Gui, Zehan Wang, Jie Chen, and Zhenyu Yue. Comprehensive Assessment of BERT-Based Methods for Predicting Antimicrobial Peptides. *Journal of Chemical Information and Modeling*, 64(19):7772–7785, 2024. PMID: 39316765.
 16. Simon Geisler, Arthur Kosmala, Daniel Herbst, and Stephan Günnemann. Spatio-Spectral Graph Neural Networks. In *The Thirty-eighth Annual Conference on Neural Information Processing Systems*, 2024.
 17. Pierre Geurts, Damien Ernst, and Louis Wehenkel. Extremely randomized trees. *Machine Learning*, 63:3–42, 2006.
 18. Montserrat Goles, Anamaría Daza, Gabriel Cabas-Mora, Lindybeth Sarmiento-Varón, Julieta Sepúlveda-Yañez, Hoda Anvari-Kazemabad, Mehdi D Davari, Roberto Uribe-Paredes, Álvaro Olivera-Nappa, Marcelo A Navarrete, and David Medina-Ortiz. Peptide-based drug discovery through artificial intelligence: towards an autonomous design of therapeutic peptides. *Briefings in Bioinformatics*, 25(4):bbae275, 06 2024.
 19. Will Hamilton, Zhitao Ying, and Jure Leskovec. Inductive Representation Learning on Large Graphs. *Advances in Neural Information Processing Systems*, 30, 2017.
 20. Xiaoxin He, Bryan Hooi, Thomas Laurent, Adam Perold, Yann LeCun, and Xavier Bresson. A Generalization of ViT/MLP-Mixer to Graphs. In *International Conference on Machine Learning*, pages 12724–12745. PMLR, 2023.
 21. Valentín Iglesias, Oriol Bárcenas, Carlos Pintado-Grima, Michał Burdukiewicz, and Salvador Ventura. Structural information in therapeutic peptides: Emerging applications in biomedicine. *FEBS Open Bio*, 15(2):254–268, 2025.
 22. Dejun Jiang, Zhenxing Wu, Chang-Yu Hsieh, Guangyong Chen, Ben Liao, Zhe Wang, Chao Shen, Dongsheng Cao, Jian Wu, and Tingjun Hou. Could graph neural networks learn better molecular representation for drug discovery? A comparison study of descriptor-based and graph-based models. *Journal of Cheminformatics*, 13(1):12, Feb 2021.
 23. Yan Kang, Huadong Zhang, Xinchao Wang, Yun Yang, and Qi Jia. Mmdb: Multimodal dual-branch model for multi-functional bioactive peptide prediction. *Analytical Biochemistry*, 690:115491, 2024.
 24. Guolin Ke, Qi Meng, Thomas Finley, Taifeng Wang, Wei Chen, Weidong Ma, Qiwei Ye, and Tie-Yan Liu. LightGBM: A Highly Efficient Gradient Boosting Decision Tree. In I. Guyon, U. Von Luxburg, S. Bengio, H. Wallach, R. Fergus, S. Vishwanathan, and R. Garnett, editors, *Advances in Neural Information Processing Systems*, volume 30. Curran Associates, Inc., 2017.
 25. Thomas N. Kipf and Max Welling. Semi-Supervised Classification with Graph Convolutional Networks. In *International Conference on Learning Representations (ICLR)*, 2017.
 26. Yuxiao Lai, Cao Xie, Zheng Zhang, Weiyue Lu, and Jiandong Ding. Design and synthesis of a potent peptide containing both specific and non-specific cell-adhesion motifs. *Biomaterials*, 31(18):4809–4817, 2010.
 27. Travis J Lawrence, Dana L Carper, Margaret K Spangler, Alyssa A Carrell, Tomás A Rush, Stephen J Minter, David J Weston, and Jessy L Labbé. amPEPpy 1.0: a portable and accurate antimicrobial peptide prediction tool. *Bioinformatics*, 37(14):2058–2060, 2021.
 28. Hansol Lee, Songyeon Lee, Ingo Lee, and Hojung Nam. AMP-BERT: Prediction of antimicrobial peptide function based on a BERT model. *Protein Science*, 32(1):e4529, 2023.
 29. Zeming Lin, Halil Akin, Roshan Rao, Brian Hie, Zhongkai Zhu, Wenting Lu, Nikita Smetanin, Robert Verkuil, Ori Kabeli, Yaniv Shmueli, Allan dos Santos Costa, Maryam Fazel-Zarandi, Tom Sercu, Salvatore Candido, and Alexander Rives. Evolutionary-scale prediction of atomic-level protein structure with a language model. *Science*, 379(6637):1123–1130, 2023.
 30. Yuankai Luo, Hongkang Li, Lei Shi, and Xiao-Ming Wu. Enhancing Graph Transformers with Hierarchical Distance Structural Encoding. In *The Thirty-eighth Annual Conference on Neural Information Processing Systems*, 2024.
 31. Liheng Ma, Chen Lin, Derek Lim, Adriana Romero-Soriano, Puneet K Dokania, Mark Coates, Philip Torr, and Ser-Nam Lim. Graph Inductive Biases in Transformers without Message Passing. In *International Conference on Machine Learning*, pages 23321–23337. PMLR, 2023.
 32. Yue Ma, Zhengyan Guo, Binbin Xia, Yuwei Zhang, Xiaolin Liu, Ying Yu, Na Tang, Xiaomei Tong, Min Wang, Xin Ye, et al. Identification of antimicrobial peptides from the human gut microbiome using deep learning. *Nature Biotechnology*, 40(6):921–931, 2022.
 33. Ramaswamy Nilakantan, Norman Bauman, J Scott Dixon, and R Venkataraghavan. Topological torsion: a new molecular descriptor for SAR applications. Comparison with other

- descriptors. *Journal of Chemical Information and Computer Sciences*, 27(2):82–85, 1987.
34. Philipp Probst, Anne-Laure Boulesteix, and Bernd Bischl. Tunability: Importance of Hyperparameters of Machine Learning Algorithms. *Journal of Machine Learning Research*, 20(53):1–32, 2019.
35. Ladislav Rampásek, Michael Galkin, Vijay Prakash Dwivedi, Anh Tuan Luu, Guy Wolf, and Dominique Beaini. Recipe for a General, Powerful, Scalable Graph Transformer. *Advances in Neural Information Processing Systems*, 35:14501–14515, 2022.
36. Sereina Riniker and Gregory A. Landrum. Open-source platform to benchmark fingerprints for ligand-based virtual screening. *Journal of Cheminformatics*, 5(1):26, May 2013.
37. David Rogers and Mathew Hahn. Extended-Connectivity Fingerprints. *Journal of Chemical Information and Modeling*, 50(5):742–754, 2010.
38. Célio Dias Santos-Júnior, Shaojun Pan, Xing-Ming Zhao, and Luis Pedro Coelho. Macrel: antimicrobial peptide screening in genomes and metagenomes. *PeerJ (San Francisco, CA)*, 8:e10555–e10555, 2020.
39. Erin E Schexnaydre, Jana Gerstmeier, Ulrike Garscha, Paul M Jordan, Oliver Werz, and Marcia E Newcomer. A 5-lipoxygenase-specific sequence motif impedes enzyme activity and confers dependence on a partner protein. *Biochimica et Biophysica Acta (BBA)-Molecular and Cell Biology of Lipids*, 1864(4):543–551, 2019.
40. Katarzyna Sidorczuk, Przemysław Gagat, Filip Pietluch, Jakub Kała, Dominik Rafacz, Laura Bąkała, Jadwiga Slowik, Rafał Kolenda, Stefan Rödiger, Legana C H W Fingerhut, Ira R Cooke, Paweł Mackiewicz, and Michał Burdukiewicz. Benchmarks in antimicrobial peptide prediction are biased due to the selection of negative data. *Briefings in Bioinformatics*, 23(5):bbac343, 08 2022.
41. Sebastian Spänig, Siba Mohsen, Georges Hattab, Anne-Christin Hauschild, and Dominik Heider. A large-scale comparative study on peptide encodings for biomedical classification. *NAR Genomics and Bioinformatics*, 3(2):lqab039, 05 2021.
42. Paulina Szymczak, Marcin Możejko, Tomasz Grzegorzek, Radosław Jurczak, Marta Bauer, Damian Neubauer, Karol Sikora, Michał Michalski, Jacek Sroka, Piotr Setny, Wojciech Kamysz, and Ewa Szczurek. Discovering highly potent antimicrobial peptides with deep generative model hydramp. *Nature Communications*, 14(1):1453, Mar 2023.
43. Xiaorong Tan, Qianhui Liu, Yanpeng Fang, Yingli Zhu, Fei Chen, Wenbin Zeng, Defang Ouyang, and Jie Dong. Predicting peptide permeability across diverse barriers: A systematic investigation. *Molecular Pharmaceutics*, 21(8):4116–4127, Aug 2024.
44. Roberto Todeschini and Viviana Consonni. *Molecular descriptors for chemoinformatics: volume I: alphabetical listing/volume II: appendices, references*. John Wiley & Sons, 2009.
45. Jan Tönshoff, Martin Ritzert, Eran Rosenbluth, and Martin Grohe. Where Did the Gap Go? Reassessing the Long-Range Graph Benchmark. *Transactions on Machine Learning Research*, 2024.
46. Daniel Veltri, Uday Kamath, and Amarda Shehu. Deep learning improves antimicrobial peptide recognition. *Bioinformatics*, 34(16):2740–2747, 2018.
47. Lei Wang, Nanxi Wang, Wenping Zhang, Xurui Cheng, Zhibin Yan, Gang Shao, Xi Wang, Rui Wang, and Caiyun Fu. Therapeutic peptides: current applications and future directions. *Signal Transduction and Targeted Therapy*, 7(1):48, Feb 2022.
48. Jun Xia, Lecheng Zhang, Xiao Zhu, Yue Liu, Zhangyang Gao, Bozhen Hu, Cheng Tan, Jiangbin Zheng, Siyuan Li, and Stan Z Li. Understanding the Limitations of Deep Models for Molecular property prediction: Insights and Solutions. *Advances in Neural Information Processing Systems*, 36:64774–64792, 2023.
49. Jing Xu, Fuyi Li, André Leier, Dongxu Xiang, Hsin-Hui Shen, Tatiana T Marquez Lago, Jian Li, Dong-Jun Yu, and Jiangning Song. Comprehensive assessment of machine learning-based methods for predicting antimicrobial peptides. *Briefings in Bioinformatics*, 22(5):bbab083, 03 2021.
50. Keyulu Xu, Weihua Hu, Jure Leskovec, and Stefanie Jegelka. How Powerful are Graph Neural Networks? In *International Conference on Learning Representations*, 2019.
51. Jieli Yan, Pratiti Bhadra, Ang Li, Pooja Sethiya, Longguang Qin, Hio Kuan Tai, Koon Ho Wong, and Shirley W.I. Siu. Deep-AmPEP30: Improve Short Antimicrobial Peptides Prediction with Deep Learning. *Molecular Therapy Nucleic Acids*, 20:882–894, Jun 2020.
52. Fangyan Zhang, Ping Yang, Wenbo Mao, Chao Zhong, Jingying Zhang, Linlin Chang, Xiaoyan Wu, Hui Liu, Yun Zhang, Sanhu Gou, et al. Short, mirror-symmetric antimicrobial peptides centered on “rrr” have broad-spectrum antibacterial activity with low drug resistance and toxicity. *Acta Biomaterialia*, 154:145–167, 2022.
53. Yue Zhang, Jianyuan Lin, Lianmin Zhao, Xiangxiang Zeng, and Xiangrong Liu. A novel antibacterial peptide recognition algorithm based on BERT. *Briefings in Bioinformatics*, 22(6):bbab200, 05 2021.

Supplementary information

Reproducibility and hardware details

To ensure the full reproducibility of our results, we used `uv` to pin the exact version of all dependencies in the project, including transitive dependencies of directly used libraries. We distribute the `pyproject.toml` and resulting `uv.lock` file with our source code. This ensures the exact reproducibility of all results that is OS-agnostic and hardware-agnostic.

We conduct experiments primarily on CPU, as our method does not require GPU. Only for ESM2 we used NVidia RTX 3080 GPU with 12 GB VRAM. All experiments were run on a machine with Intel Core i7-12700KF 3.61 GHz CPU and 96 GB RAM, running Linux Ubuntu 24.04 OS. We additionally ran the experiments on a second machine with Intel Core i7-10850H 2.70 GHz CPU and 32 GB RAM, running Linux Ubuntu 22.04 OS. The results were exactly the same in all cases.

Targets in specific benchmarks

Here we describe in detail targets of each benchmark.

AMPBenchmark

In AMPBenchmark [40] authors focus on one task, which is antimicrobial activity. The dataset includes a test set consisting of 5 repeats and multiple training sets, each also consisting of 5 repeats. All training sets and their repeats use the same 4151 samples as their entire positive class, and all repeats of the test set use the same 1039 positive samples similarly. Repeats and training sets differ by the negatives sampling method, as described in the main body.

Each training set is defined by a sampling method used to chose negative class samples. The samples vary by number and length distribution. We report the distributions of sequence length for positive class and for negative class generated by each method in Figure 5. We also report the number of unique samples generated by each method and average number of common samples within two different repeats of the same method in Table 9.

Table 9. AMPBenchmark negative class counts and average common sample count off different subsampling methods.

Sampling method	Unique samples	Avg. common samples count
Gabere&Noble	124504	1.7
dbAMP	5138	3285.8
CS-AMPPred	5829	2942.3
Wang-et-al	41784	0.1
Witten&Witten	20754	0.1
AMAP	20046	0
ampir-mature	3579	2285
iAMP-2L	7327	4678.3
AmpGram	20754	0.1
AMPScannerV2	20755	0
AMPLify	20752	0.1

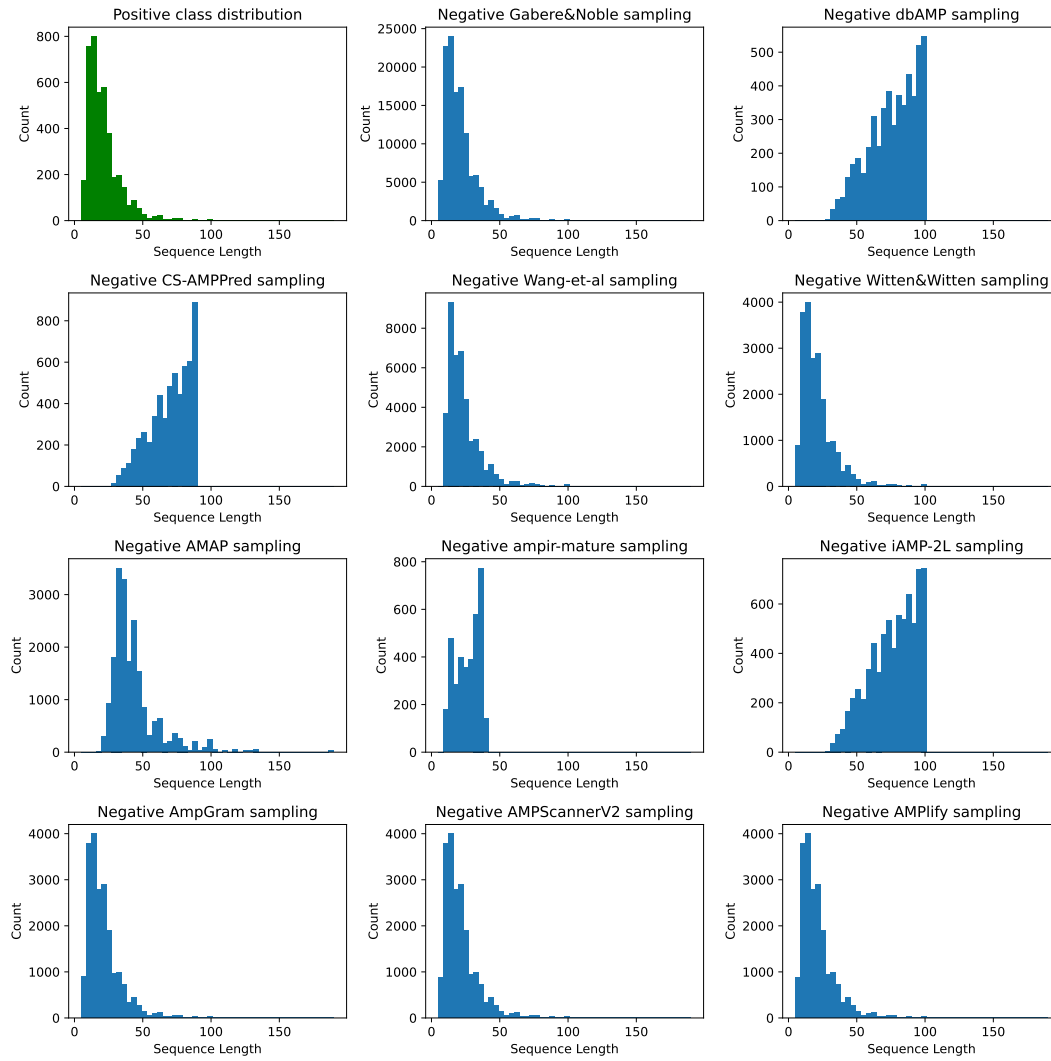


Fig. 5: AMPBenchmark [40] sequence length distributions for different negative sampling methods.

AutoPeptideML

In AutoPeptideML [12], authors use 16 independent tasks predicting targets to assess predictive performance against varied biological endpoints. Each classification task is almost perfectly balanced. These tasks include: antibacterial activity, ACE inhibition, anticancer activity, antifungal activity, antimalarial activity, antimicrobial activity, antioxidant activity, antiparasitic activity, antiviral activity, blood-brain barrier penetration, DPPIV inhibition, anti-MRSA activity, neuropeptide activity, quorum sensing activity, toxicity prediction, and tumor T-cell antigen identification.

We report sequence length distributions for each task in Figure 6. We additionally report the number of train and test samples for each of the targets in Table 10.

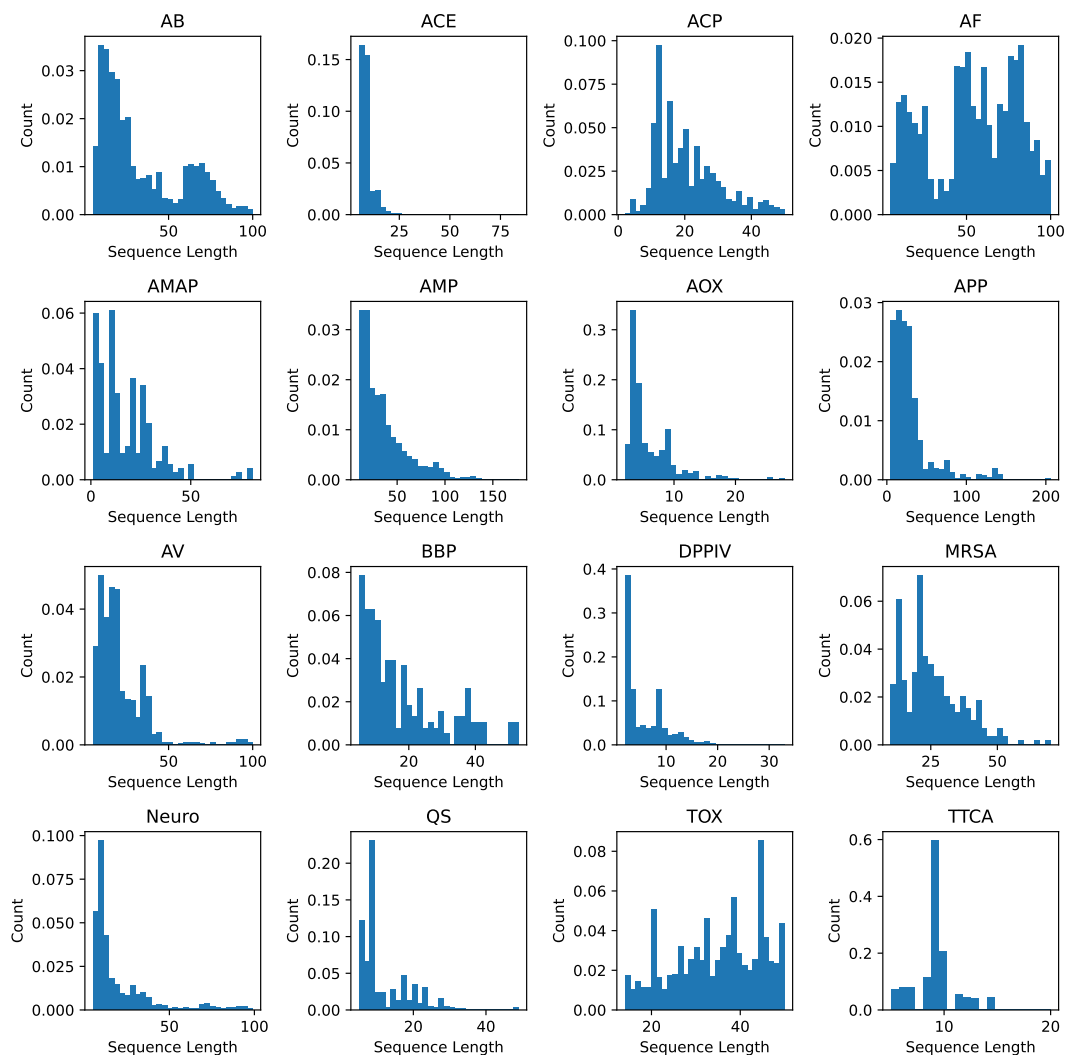


Fig. 6: AutoPeptideML [12] sequence length distribution across different datasets.

Table 10. Dataset sizes in AutoPeptideML [12].

Target	Train size	Test size
AB	13245	3311
ACE	1685	421
ACP	1378	344
AF	1591	395
AMAP	221	55
AMP	10266	2566
AOX	698	174
APP	482	120
AV	4711	1177
BBP	191	47
DPPIV	1063	265
MRSA	237	59
Neuro	3881	969
QS	349	87
TOX	3092	772
TTCA	948	236

BERT-based models benchmark

In BERT-based models benchmark [15] authors focus on antimicrobial peptides (AMPs) classification using 6 different datasets. As described in the main body, BERT models are pretrained, and whole datasets are used for testing in the aforementioned publication. To mimic this with our approach, we use a leave-one-dataset-out strategy. For example, when evaluating on the ADAPTABLE dataset, we merge all remaining datasets into a single training set and apply CD-HIT-2D [14] at a 40% threshold to remove peptides overly similar to those in the test set.

This approach creates 6 new datasets, with the original one being the test set, and all others, after CD-HIT-2D, become the training set. We summarize the sequence length distributions of resulting datasets in Figure 7. We include the train and test set sizes, as well as percentage of positive class for each task, in Table 11. Training sets have different positive class percentage due to the applied procedure, but test sets are exactly the same, original datasets, as used in [15], and have 50% negative and positive class.

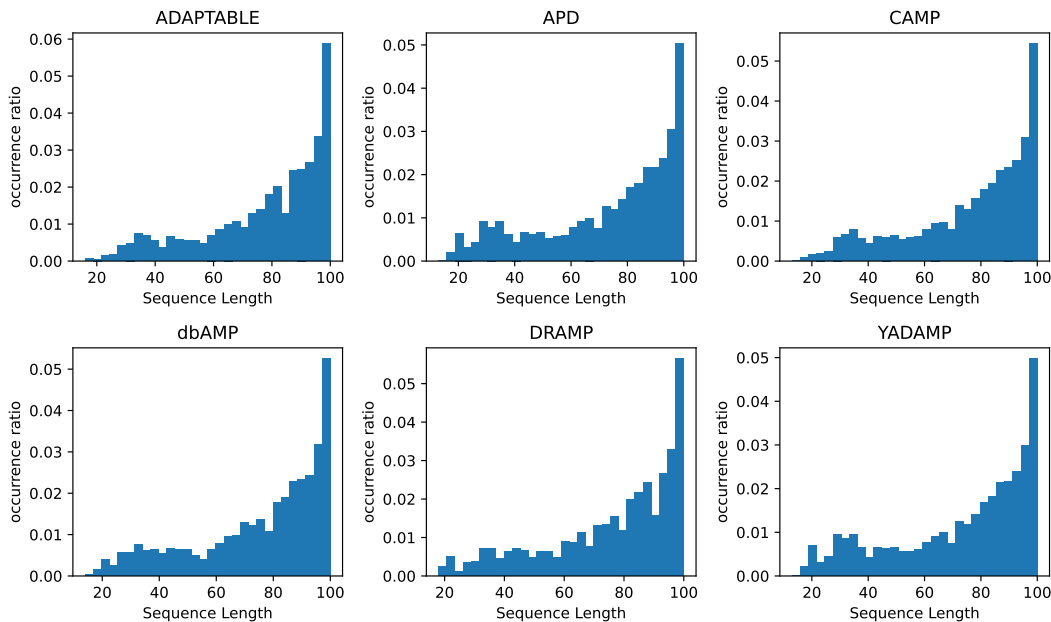


Fig. 7: BERT AMP Benchmark [15] sequence length distribution across different datasets.

Table 11. Dataset sizes in BERT-based models benchmark [15].

Dataset	Train size	Train positive class %	Test size	Test positive class %
ADAPTABLE	2282	36.33%	2170	50.00%
APD	5887	49.26%	68	50.00%
CAMP	3773	43.97%	1154	50.00%
dbAMP	4905	47.46%	568	50.00%
DRAMP	2731	45.26%	2082	50.00%
YADAMP	5978	49.75%	46	50.00%

PeptideReactor

PeptideReactor [41] is a large benchmark including 50 binary classification datasets. Their tasks include A-cell epitope classification, three anticancer tasks, two antifungal tasks, two anti-inflammatory tasks, seven antimicrobial tasks, two antibacterial tasks, two antiviral tasks, linear B-cell epitope classification, eight cell-penetrating tasks, hemolytic activity classification, seventeen HIV-related tasks, immunosuppressive activity based on IL-10 induction, insect neuropeptide classification, proinflammatory activity classification, and T-cell epitope classification, all formulated as binary classification tasks.

We report sequence length distribution for each of these tasks in Figure 8. It is worth noting that many of the tasks are fixed on a specific sequence length for the entire dataset. Train-test splits are not provided for the benchmark, as it uses 10 repetitions of 5-fold cross-validation. In Table 12, we report: size of each dataset, positive class percentage, and statistics of sequence length distribution (not plots due to large number of datasets).

Table 12. Dataset sizes in PeptideReactor[41].

Dataset	Dataset size	Positive class %	Sequence length						
			min	p5	p25	median	p75	p95	max
ace_vaxinpad	688	44.04%	3	4	5	10	17	26	30
acp_anticip	450	50.00%	5	7	15	25	34	49	113
acp_iacp	344	40.12%	11	13	18	25	30	38	97
acp_mlacp	585	31.97%	11	13	20	25	32	45	50
afp_amppred	2768	50.00%	10	13	19	26	37	67	255
afp_antifp	2916	50.03%	4	12	41	55	73	94	100
aip_aippred	1049	40.04%	11	15	15	15	18	20	25
aip_antiinflam	2124	40.63%	7	9	15	15	19	21	30
amp_antibp	861	50.06%	30	30	30	30	30	30	30
amp_antibp2	1993	50.13%	6	13	20	27	37	53	94
amp_csamp	256	50.00%	16	29	34	47	85	110	119
amp_fernandes	231	49.78%	11	18	32	41	63	92	100
amp_gonzales	129	20.93%	11	14	20	26	38	55	84
amp_iamp2l	3284	26.77%	5	13	32	65	86	98	103
amp_modlamp	2579	47.50%	30	30	35	40	46	73	100
atb_antitbp	492	50.00%	5	7	9	12	20	38	61
atb_iantitb	492	50.00%	5	6	9	12	19	38	61
avp_amppred	1478	50.00%	10	12	17	22	34	39	255
avp_avppred	1047	57.21%	6	8	15	20	30	37	107
bce_ibce	2518	44.08%	11	12	15	15	18	22	49
cpp_cellppd	1614	50.00%	3	6	12	17	25	34	61
cpp_cellppdmod	1462	50.07%	3	7	12	16	21	30	41
cpp_cppredfl	924	50.00%	10	11	14	18	26	37	61
cpp_kelmcpp	1003	50.25%	8	12	15	19	25	30	49
cpp_mixed	128	75.78%	5	7	13	16	21	27	38
cpp_mlcpp	1903	38.78%	5	10	14	19	26	34	48
cpp_mlcppue	374	50.00%	5	7	11	15	18	27	61
cpp_sanders	145	76.55%	5	7	15	18	22	27	43
hem_hemopi	1104	47.28%	4	11	14	18	25	34	98
hiv_3tc	624	31.25%	141	240	240	241	242	245	249
hiv_abc	619	28.92%	31	240	240	241	242	245	249
hiv_apv	702	60.40%	99	99	99	99	100	102	107
hiv_azt	621	51.85%	141	240	240	241	242	245	249
hiv_bevirimat	155	27.74%	19	20	21	21	21	21	21
hiv_d4t	621	54.11%	31	240	240	241	242	245	249
hiv_ddi	623	49.12%	141	240	240	241	242	245	249
hiv_dlv	718	63.37%	170	240	240	241	242	246	253
hiv_efv	721	62.00%	74	240	240	241	242	246	253
hiv_idv	758	50.66%	99	99	99	99	100	102	107
hiv_lpv	501	44.51%	99	99	99	99	100	102	107
hiv_nfv	775	39.10%	99	99	99	99	100	102	107
hiv_nvp	733	56.62%	170	240	240	241	242	246	253
hiv_protease	947	15.73%	8	8	8	8	8	8	8
hiv_rtv	728	47.94%	99	99	99	99	100	102	107
hiv_sqv	761	60.05%	99	99	99	99	100	102	107
hiv_v3	1351	14.80%	32	34	35	35	35	35	38
isp_il10pred	1242	31.72%	8	13	15	15	15	20	42
nep_neuropipred	1750	50.00%	4	10	14	20	31	77	100
pip_pipel	3228	25.81%	11	15	15	15	15	20	25
tce_zhao	203	17.73%	10	10	10	10	10	10	10

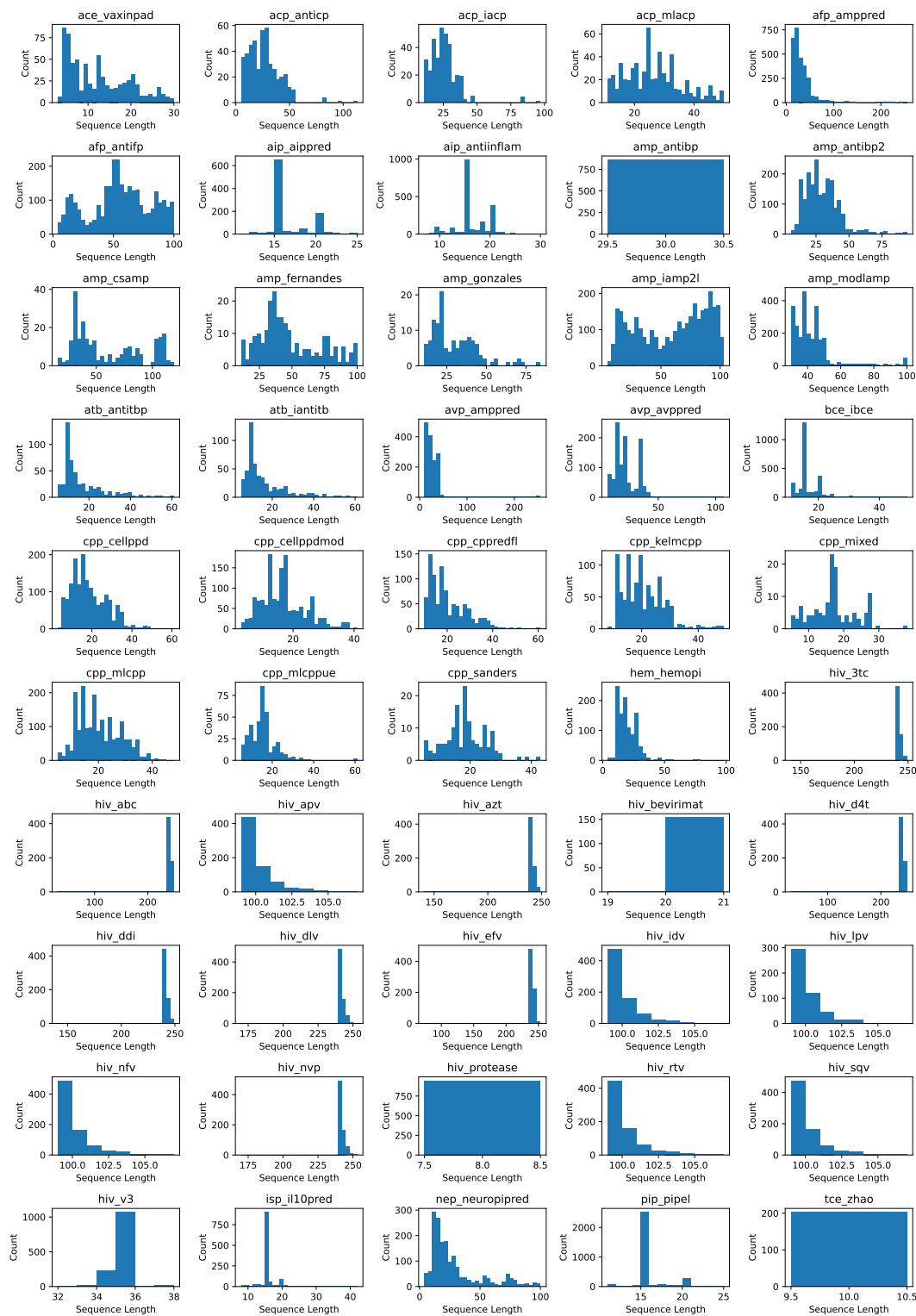


Fig. 8: PeptideReactor [41] sequence length distribution across different tasks.

XUAMP

Authors of XUAMP [49] focus solely on antimicrobial peptides. The training part of this one dataset consists of 11072 samples, and testing part of 3072 samples. Both of these subsets have balanced class labels, with 50% positive and negative samples. We report the sequence length distribution from this dataset in Figure 9.

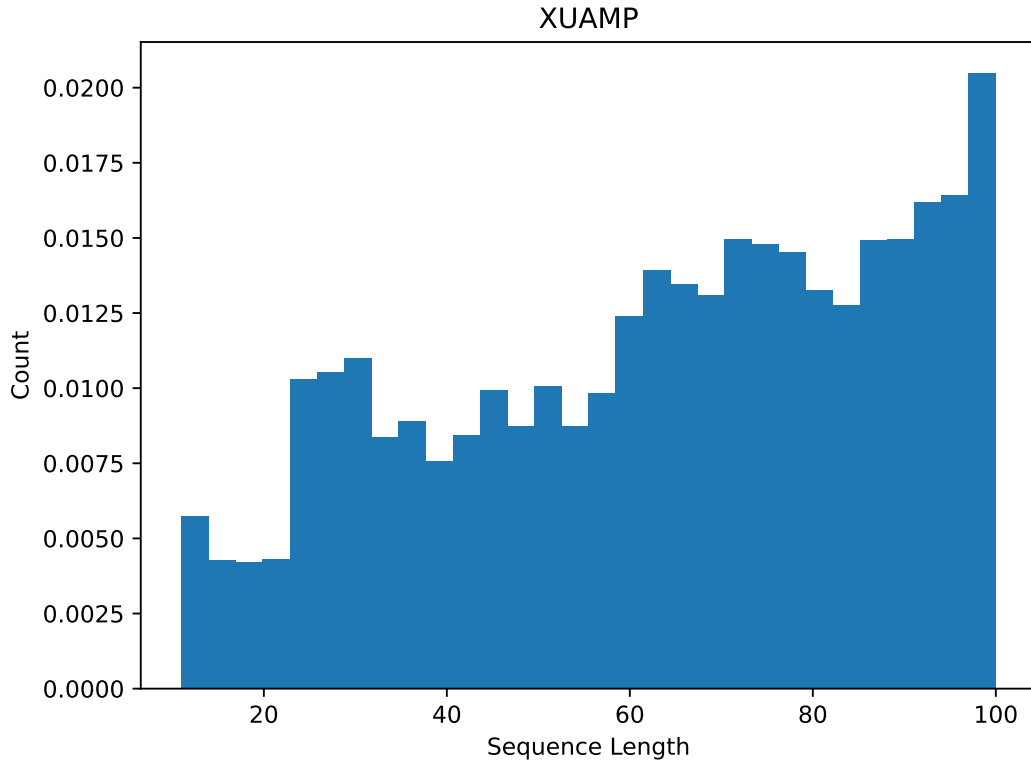


Fig. 9: XUAMP [49] sequence length distribution.

LRGB

Long-Range Graph Benchmark (LRGB) [9] provides multiple datasets, of which we use Peptides-func and Peptides-struct in this work. They have the same peptides, but different labels (classification vs regression). Both datasets contain the same 13204 samples in the training and 2331 in the test set.

We note that LRGB provides valid SMILES for all peptides, but some sequences contain custom notation for chemically modified amino acids. This cannot be parsed by, e.g., ESM or amino acid counts baselines, and also cannot be used for shuffling experiments. Thus, we exclude those sequences for those cases. However, only 125 training sequences and 20 test sequences are removed this way. Based on the remaining, valid sequences we report distribution of sequence lengths as shown in Figure 10

For peptides-func the tasks include antifungal activity, cell-cell communication, anticancer activity, drug delivery vehicle functionality, antimicrobial activity, antiviral activity, antihypertensive activity, antibacterial activity, antiparasitic activity, and toxicity prediction.

For peptides-struct the targets include mass-weighted moments of inertia along principal components 1, 2, and 3, valence-weighted moments of inertia along principal components 1, 2, and 3, peptide length along the x-, y-, and z-axes, sphericity, and deviation from the best-fit plane.

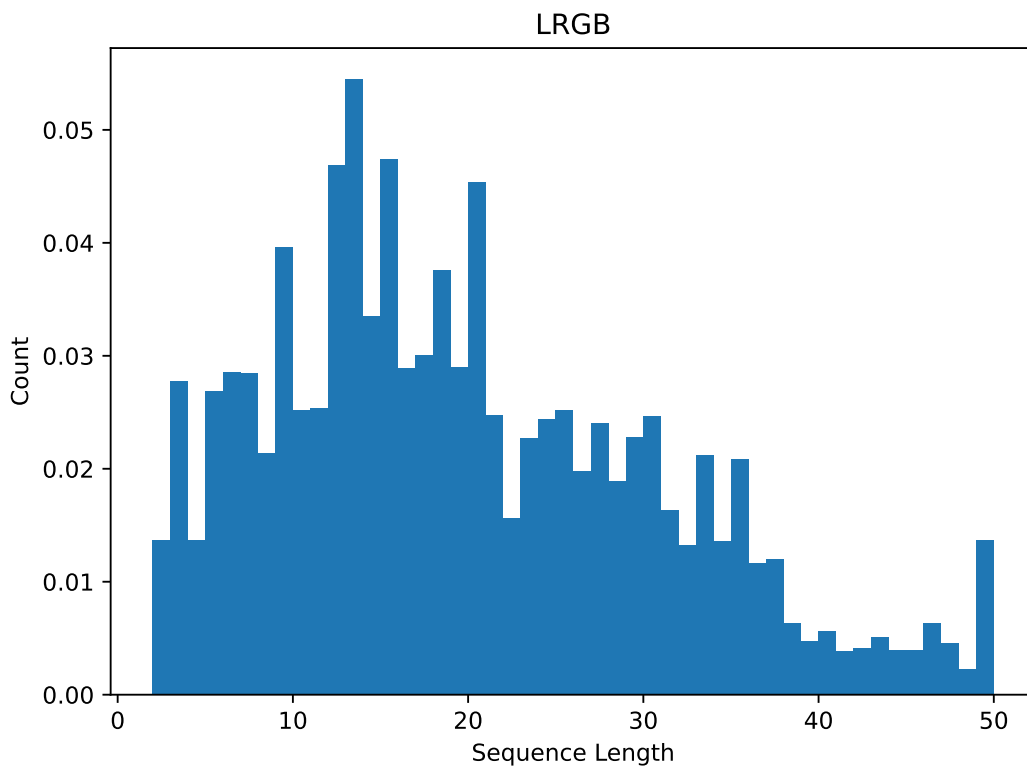


Fig. 10: LRGB peptides [9] heavy atom count distribution.

Additional benchmark metrics

Here, we report additional metrics for AMPs benchmarks from [15] (Table 13) and [49] (Table 14), as well as AutoPeptideML benchmark [12] (Table 15). They were omitted in the main text due to space limitations.

Table 13. Results for BERT benchmark [15] results.

Metric	Model	ADAPTABLE	APD	CAMP	dbAMP	DRAMP	YADAMP	avg
Recall	AMP-BERT	67.60	79.40	80.40	54.20	54.70	82.60	69.82
	Bert-Protein	58.40	94.10	76.30	83.80	47.60	47.60	67.97
	cAMPs_pred	44.50	58.80	57.90	36.30	24.70	73.90	49.35
	LM_pred	40.00	55.90	49.10	45.10	31.80	69.60	48.58
	LM_pred (BFD)	64.60	88.20	78.00	58.50	52.80	82.60	59.67
	ECFP	75.60	97.10	88.70	95.10	66.80	100.00	87.22
	TT	75.60	97.10	89.10	94.00	67.10	100.00	87.15
	RDKit	77.20	97.10	88.70	94.00	66.50	100.00	87.25
Precision	AMP-BERT	80.20	77.10	84.20	74.40	77.10	82.60	79.27
	Bert-Protein	79.20	86.50	85.40	82.10	77.10	77.10	81.23
	cAMPs_pred	98.20	100.00	97.90	94.50	94.80	100.00	97.57
	LM_pred	92.50	100.00	94.00	92.80	94.00	100.00	95.55
	LM_pred (BFD)	86.30	91.20	90.20	83.40	83.90	86.40	91.62
	ECFP	86.90	89.20	87.70	88.20	89.00	92.00	88.83
	TT	86.40	91.70	88.50	87.80	89.80	92.00	89.37
	RDKit	87.50	89.20	88.00	89.00	89.80	85.20	88.12
AUROC	AMP-BERT	81.70	91.80	90.60	78.40	76.90	90.70	85.02
	Bert-Protein	79.40	96.10	90.90	91.90	74.00	74.00	84.38
	cAMPs_pred	82.30	91.80	87.00	81.90	68.10	93.00	84.02
	LM_pred	88.00	97.20	92.30	89.50	82.80	98.70	91.42
	LM_pred (BFD)	86.30	97.40	93.60	87.60	83.90	93.40	90.47
	ECFP	89.50	98.40	94.30	97.20	87.80	100.00	94.53
	TT	89.30	98.20	94.30	97.10	87.60	100.00	94.42
	RDKit	90.20	99.30	94.80	97.00	88.20	100.00	94.92
F1	AMP-BERT	81.70	78.30	82.30	62.70	64.00	82.60	75.27
	Bert-Protein	79.40	90.10	80.60	82.90	58.80	58.80	75.10
	cAMPs_pred	61.30	74.10	72.80	52.40	39.20	85.00	64.13
	LM_pred	55.90	71.70	64.50	60.70	47.60	82.10	63.75
	LM_pred (BFD)	73.90	89.60	83.60	68.70	64.80	84.40	70.32
	ECFP	80.80	93.00	88.20	91.50	76.30	95.80	87.60
	TT	80.60	94.30	88.80	90.80	76.90	95.80	87.87
	RDKit	82.00	93.00	88.40	91.40	76.40	92.00	87.20

Table 14. Additional metrics for results on [49].

Method	Accuracy	AUROC	F1	MCC	Recall	Specificity
AMPscannerV2	56.8	58.5	54.8	0.137	52.3	61.3
iAMP-2L	59.2	59.2	36.8	0.261	23.8	94.7
ADAM-SVM	61.2	61.2	47.1	0.264	34.6	87.8
ampir	56.3	61.9	37.9	0.156	26.6	85.9
MLAMP	55.3	62.9	23	0.194	13.3	97.2
ADAM-HMM	68.4	68.4	62.3	0.39	52.1	84.7
AMPlify	64.2	69.7	46.2	0.381	30.7	97.6
AMPEP	65.8	72.7	48.7	0.425	32.5	99.2
AMPfun	67.4	73.5	55.5	0.414	40.6	94.3
RDKit	67.5	73.7	58.5	0.388	45.8	89.1
ECFP	69.3	75.3	60.9	0.426	47.9	90.6
TT	69.4	74.9	61.7	0.424	49.3	89.5

Table 15. Additional metrics for results on AutoPeptideML [12].

Model	# params	Accuracy	MCC	AUROC	F1
ProtBERT	420M	68.5	0.375	75.9	67.7
ESM2-150M	150M	69.8	0.402	77.7	68.5
Prot-T5	3B	70.0	0.409	77.1	69.0
ESM2-8M	8M	70.2	0.418	77.5	69.4
ESM2-35M	35M	71.0	0.428	78.0	70.2
ESM1b-650M	650M	71.1	0.433	78.9	69.2
ESM2-650M	650M	68.0	0.438	79.7	69.7
Prot-T5-XL	3B	68.9	0.447	79.7	70.4
RDKit	20k	70.7	0.421	76.9	69.6
TT	23k	70.8	0.422	77.1	69.4
ECFP	22k	71.5	0.437	78.1	70.2

Additional classifiers on LRGB

Here, we present results of two additional classifiers on the LRGB benchmark datasets: Random Forest and Extremely Randomized Trees [17]. For both we use 500 trees, entropy or squared error as cost function (for classification and regression, respectively), and class weighting for classification. We can report standard deviations for them over 10 random seeds, because they are nondeterministic.

Peptides-func results are in Table 16, and Peptides-struct in Table 17. For clarity, we also include LightGBM results from the main body, which is a deterministic classifier and thus does not have standard deviation.

Random Forest and Extremely Randomized Trees classifiers have very low standard deviation, highlighting the stability of the fingerprint-based approach. Models based on ECFP features consistently achieve the best results in all cases, but other fingerprints and classifiers also obtain results highly competitive with long-range GNNs.

Table 16. AUPRC \uparrow for different classifiers on Peptides-func.

	LightGBM	Random Forest	Extremely Randomized Trees
RDKit	73.11	71.48 \pm 0.13	69.38 \pm 0.06
TT	73.18	71.66 \pm 0.09	69.86 \pm 0.08
ECFP	74.60	73.55 \pm 0.10	71.98 \pm 0.08

Table 17. MAE ↓ for different classifiers on Peptides-struct.

	LightGBM	Random Forest	Extremely Randomized Trees
RDKit	0.2459	0.2459 ± 0.0002	0.2440 ± 0.0001
TT	0.2438	0.2471 ± 0.0003	0.2467 ± 0.0003
ECFP	0.2432	0.2442 ± 0.0002	0.2433 ± 0.0001

Additional LRGB timings

Here, we present expanded timings of fingerprints and compare them to times reported in LRGB [9] (Appendix C.2), summarizing them in Table 18. Times for fingerprint-based models are an average of 10 runs on 12-core Intel Core i7-12700KF. We measure them for *Peptides-func*, and for *Peptides-struct* results were almost identical. Timings for GNNs are taken from [9], and use Nvidia A100 GPU.

The entire time for our approach (feature extraction + classifier training) is shorter than precomputing structural embeddings or training even a single epoch of SAN model. Graph transformer model has faster epochs, they still require precomputing LapPE embeddings, while also giving much worse results than fingerprints (see main body for results table).

One should also take into consideration the difference in raw compute power (CPU vs powerful GPU) required to get those times, which makes the difference even more significant.

Table 18. Time of computation on Peptides-func.

Model	Time [s]
Transformer+LapPE	5.9
SAN+LapPE	53.6
SAN+RWSE	49.7
LapPE encoding	74
RWSE encoding	53
ECFP	19
TT	15.2
RDKit	42.8

Additional PeptideReactor results

Here, we present the performance of all encodings on PeptideReactor [41], in Table 19. They are sorted from highest to lowest result. Further, in Table 20, we provide results for molecular fingerprints with and without tuning their hyperparameters.

Table 19. Full results on PeptideReactor benchmark [41].

Encoding	Avg F1	Type
FP encoding	82.9	fingerprint
cksaap	82.4	sequence
dist_f	82.2	sequence
psekraac	81.8	sequence
ECFP	81.7	fingerprint
ngram_	81.6	sequence
dde	81.3	sequence
dpc	80.6	sequence
TT	80.6	fingerprint
RDKit	80.6	fingerprint
fldpc_	79.4	sequence
qsorde	78.9	sequence
waac_a	78.8	sequence
apaac_	78.2	sequence
aac	78.1	sequence
binary	77.9	sequence
ctdd	77.9	sequence
paac_l	77.9	sequence
aainde	77.8	sequence
tpc	76.6	sequence
cksaag	76.5	sequence
ctriad	75.9	sequence
ctdt	75.7	sequence
ctdc	75.6	sequence
ksctri	75.6	sequence
gtpc	75	sequence
gdpc	74	sequence
figc_a	73.8	sequence
fft_aa	73.3	sequence
qsar	72.8	structure
nmbrot	72.3	sequence
zscale	72.1	sequence
eaac_w	71.6	sequence
blomap	70.9	sequence
egaac_	70.3	sequence
blosum	69.8	sequence
delaun	69.5	structure
gaac	69.5	sequence
moran_	69	sequence
socnum	69	sequence
geary_	68.9	sequence
cgr_re	68.8	sequence
distan	61.3	structure
electr	60.9	structure
disord	53.5	structure
sseb	51.7	structure
asa	51.5	structure
ta	51.4	structure
ssec	48.3	structure

Table 20. Results on PeptideReactor benchmark [41] with and without tuning.

Fingerprint	Tuned?	F1 score
ECFP	No	79.4%
	Yes	81.7%
Topological Torsion	No	77.8%
	Yes	80.6%
RDKit	No	80.0%
	Yes	80.6%

Shuffling results

Here we report additional sequence shuffling experiments. We evaluate the performance of three models for different shuffling ratios: molecular fingerprints ECFP model, amino acid counts, and ESM2. For each benchmark and model we perform two distinct experiments. In one, we shuffle only sequences from the train set, and in the other from both train and test set.

We present results for individual models in Figures 11, 12 and 13. Comparisons of those models within each benchmark are reported in Tables 21, 22, 23, 24 and 25. Results include the performance loss delta, computed as the difference between performance achieved with unshuffled and fully shuffled data.

For both variants of the experiment, our ECFP model maintains comparable performance regardless of shuffling ratio, showing only a slight decrease compared to other models. Amino acid count model performs consistently only on AutoPeptideML, BERT AMP and XUAMP. Degradation in performance of sequence-based baselines is particularly prominent for LRGB and PeptideReactor. We can see that the two baseline models perform worse in the unshuffled test set experiment. Our hypothesis is that this induces a distribution shift between shuffled train and unshuffled test sequences, resulting in quality degradation.

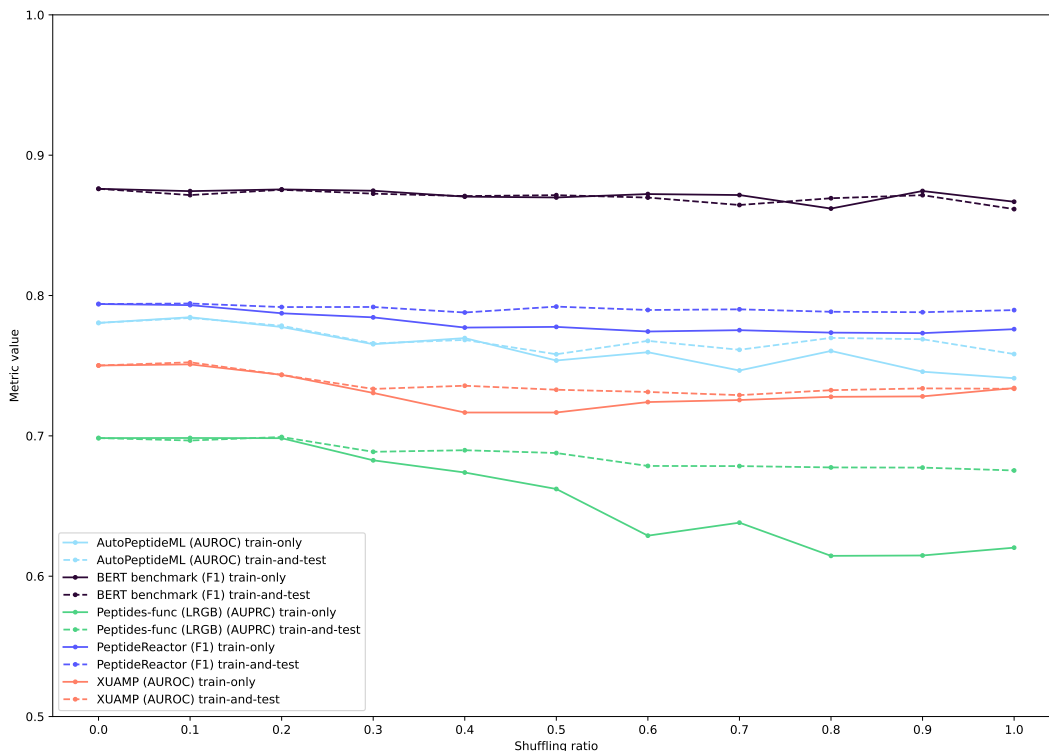


Fig. 11: Shuffling metrics for ECFP + LightGBM.

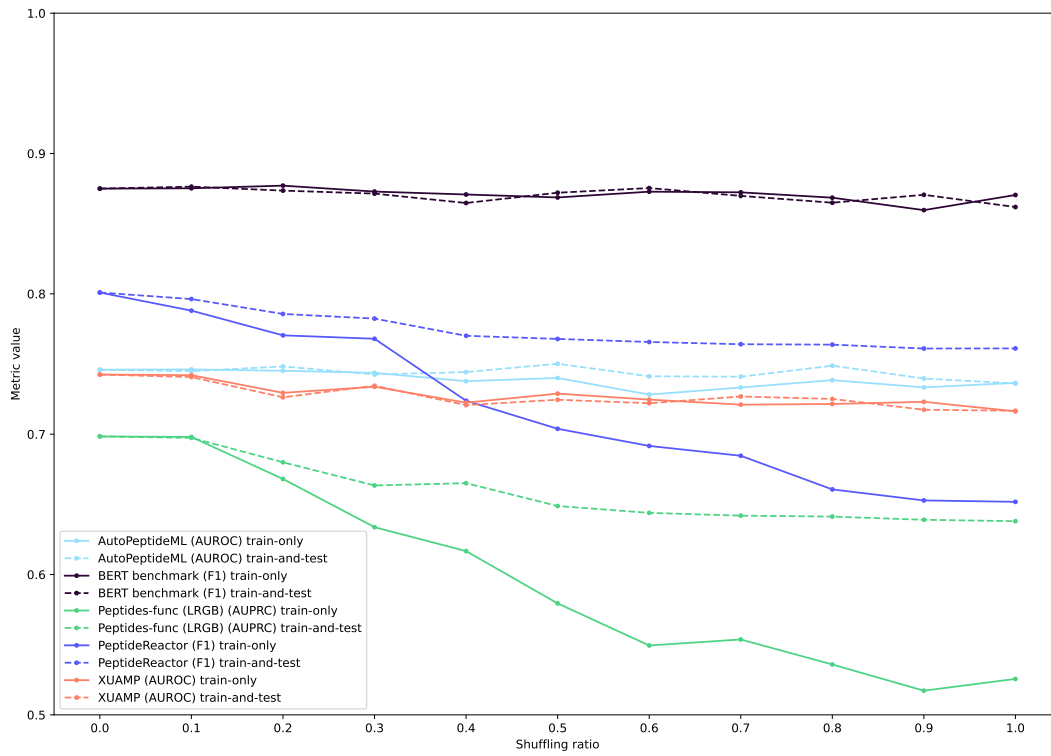


Fig. 12: Shuffling metrics for amino acid counts model.

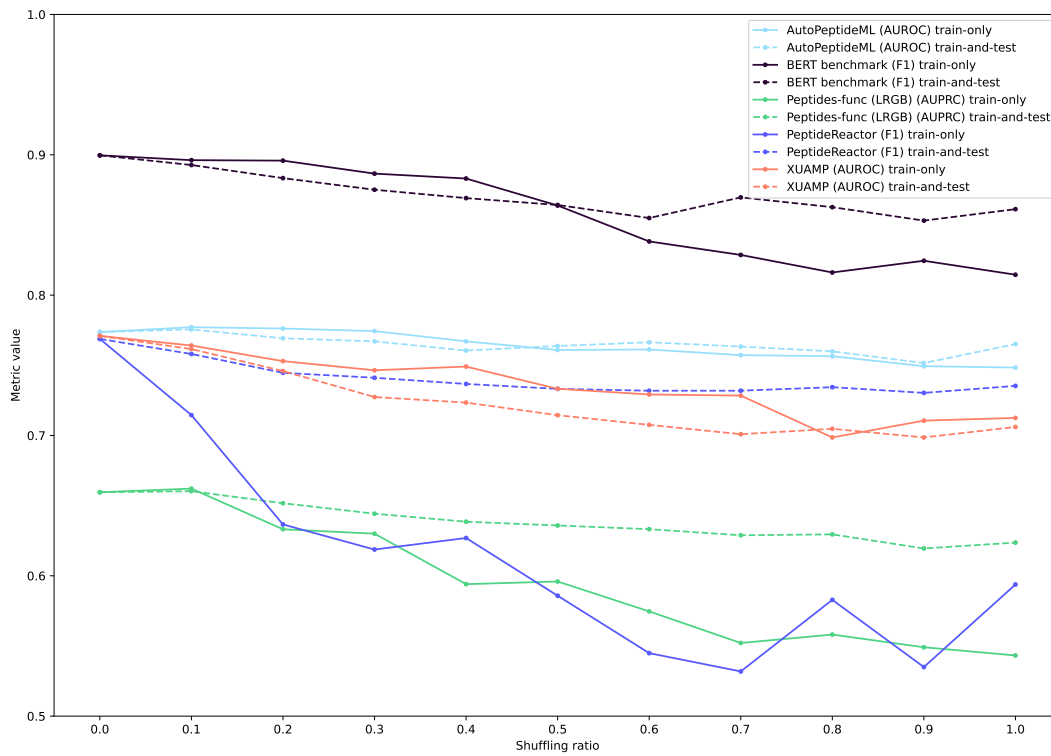


Fig. 13: Shuffling metrics for ESM2 [29].

Table 21. Shuffling results for AutoPeptideML [12], AUROC metric.

Shuffle ratio	ECFP		Amino acid counts		ESM2	
	train	train and test	train	train and test	train	train and test
0.0	78.05	78.05	74.59	74.59	77.37	77.37
0.1	78.45	78.4	74.61	74.49	77.71	77.56
0.2	77.76	77.85	74.52	74.83	77.62	76.93
0.3	76.53	76.59	74.37	74.26	77.44	76.71
0.4	76.97	76.84	73.78	74.43	76.71	76.05
0.5	75.37	75.82	74.00	75.02	76.09	76.38
0.6	75.96	76.77	72.82	74.12	76.13	76.64
0.7	74.66	76.13	73.33	74.10	75.72	76.34
0.8	76.05	76.98	73.85	74.88	75.65	75.99
0.9	74.57	76.89	73.34	73.97	74.94	75.16
1.0	74.11	75.83	73.65	73.61	74.84	76.51
delta	-3.94	-2.22	-0.94	-0.98	-2.53	-0.86

Table 22. Shuffling results for BERT-based models benchmark [15], F1 metric.

Shuffle ratio	ECFP		Amino acid counts		ESM2	
	train	train and test	train	train and test	train	train and test
0.0	87.61	87.61	87.5	87.5	89.96	89.96
0.1	87.44	87.16	87.52	87.64	89.62	89.27
0.2	87.56	87.53	87.71	87.36	89.58	88.34
0.3	87.47	87.26	87.29	87.14	88.66	87.51
0.4	87.05	87.09	87.08	86.47	88.31	86.91
0.5	86.99	87.15	86.87	87.21	86.39	86.42
0.6	87.23	86.98	87.28	87.54	83.83	85.49
0.7	87.16	86.45	87.23	86.98	82.86	86.97
0.8	86.20	86.93	86.85	86.49	81.62	86.27
0.9	87.45	87.15	85.97	87.06	82.45	85.31
1.0	86.68	86.16	87.04	86.19	81.46	86.12
delta	-0.93	-1.45	-0.46	-1.31	-8.50	-3.84

Table 23. Shuffling results for LRGB Peptides-func benchmark [9], AUPRC metric.

Shuffle ratio	ECFP		Amino acid counts		ESM2	
	train	train and test	train	train and test	train	train and test
0.0	92.09	92.09	91.02	91.02	90.74	90.74
0.1	91.73	91.72	90.96	91.04	90.40	90.36
0.2	91.78	91.94	89.89	90.55	89.55	90.52
0.3	91.03	91.15	89.58	90.47	88.69	89.76
0.4	90.83	91.24	87.81	89.14	86.72	89.74
0.5	90.61	91.56	86.46	88.76	86.83	89.32
0.6	90.41	91.91	85.99	88.70	86.73	89.26
0.7	89.73	91.27	85.41	89.03	85.04	88.91
0.8	89.09	90.94	83.71	87.93	85.49	89.44
0.9	88.84	90.68	83.87	88.57	85.28	88.79
1.0	89.39	90.91	83.83	88.65	83.84	89.50
delta	-2.7	-1.18	-7.19	-2.37	-6.9	-1.24

Table 24. Shuffling results for PeptideReactor benchmark [41], F1 metric.

Shuffle ratio	ECFP		Amino acid counts		ESM2	
	train	train and test	train	train and test	train	train and test
0.0	79.39	79.39	80.09	80.09	76.88	76.88
0.1	79.32	79.43	78.80	79.63	71.45	75.81
0.2	78.74	79.18	77.04	78.57	63.66	74.47
0.3	78.44	79.18	76.80	78.24	61.87	74.11
0.4	77.72	78.79	72.38	77.01	62.69	73.67
0.5	77.77	79.21	70.39	76.79	58.58	73.32
0.6	77.44	78.97	69.16	76.57	54.49	73.19
0.7	77.53	79.02	68.46	76.41	53.18	73.19
0.8	77.36	78.84	66.06	76.38	58.29	73.44
0.9	77.32	78.81	65.28	76.10	53.50	73.04
1.0	77.60	78.96	65.18	76.11	59.38	73.53
delta	-1.79	-0.43	-14.91	-3.98	-17.50	-3.35

Table 25. Shuffling results for XUAMP benchmark [49], AUROC metric.

Shuffle ratio	ECFP		Amino acid counts		ESM2	
	train	train and test	train	train and test	train	train and test
0.0	75.01	75.01	74.25	74.25	77.10	77.10
0.1	75.1	75.24	74.2	74.07	76.41	76.16
0.2	74.35	74.35	72.94	72.63	75.30	74.59
0.3	73.06	73.34	73.38	73.45	74.65	72.74
0.4	71.66	73.57	72.25	72.07	74.91	72.34
0.5	71.66	73.29	72.89	72.45	73.33	71.44
0.6	72.41	73.13	72.46	72.21	72.92	70.76
0.7	72.55	72.9	72.10	72.69	72.84	70.09
0.8	72.78	73.25	72.15	72.51	69.86	70.48
0.9	72.81	73.38	72.31	71.74	71.06	69.86
1.0	73.41	73.35	71.63	71.67	71.25	70.61
delta	-1.60	-1.66	-2.62	-2.58	-5.85	-6.49

Analysis of difficult predictions and errors

To investigate whether certain data samples are systematically more difficult for the model to predict, we used the AutoPeptideML benchmark [12]. This benchmark provides multiple prediction tasks with independent datasets and challenging train-test splits.

For each dataset, we selected samples for which the absolute difference between the true class label and the predicted probability exceeded 0.9. We compared the distributions of their physicochemical properties with those of the remaining samples, with smaller error, summarized in Figure 14. Descriptors included: sequence length; counts and fractions of positively charged, negatively charged, charged, and polar amino acids, counts of cysteines, glycines, and prolines. Additionally, we use more features typical in chemoinformatics, such as molecular weight, number of heavy atoms and bonds, lipophilicity, topological polar surface area, numbers of hydrogen bond donors and acceptors, numbers of rings and number of rotatable bonds.

We use the Epps-Singleton statistical test [11] to check if there is a statistically significant difference between the two distributions for each descriptor. It was selected as we have both continuous and discrete descriptors, and this test has higher power for discrete ones than Kolmogorov-Smirnov. Because the number of high-error samples is much smaller than the remaining samples, we repeated the test 100 times using the full high-error set and bootstrap samples of the remaining data matched in size.

Out of 16 AutoPeptideML datasets (tasks), only 3 showed statistically significant differences in any feature, and no feature was consistently significant across tasks. We additionally aggregated prediction errors across the entire benchmark and repeated the analysis, which again revealed no statistically meaningful differences between the distributions of the worst predictions and the remaining samples.

Overall, these results indicate that no individual physicochemical property consistently increases prediction difficulty when using fingerprint-based representations.

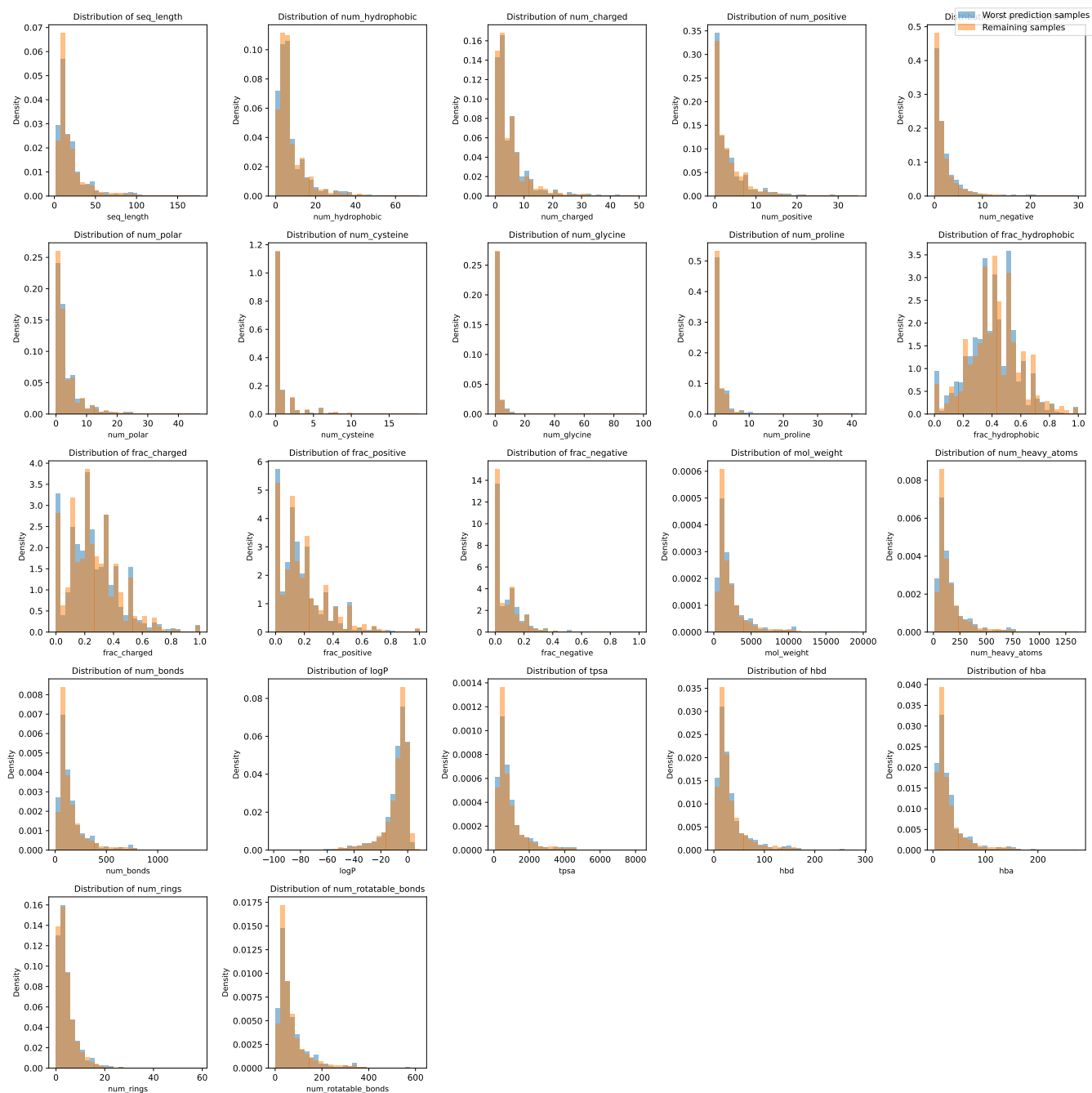


Fig. 14: AutoPeptideML [12] feature distributions.

Sequence length split

To evaluate robustness of models to length of training and testing data, we use sequence length split. We selected 3 datasets for this experiment: AutoPeptideML, Peptides-func from LRGB, and XUAMP, and we test 3 models: ECFP, amino acid counts, and ESM2.

Peptides in each dataset are sorted by sequence length and divided into 5 length buckets: 20% of the shortest ones, those of lengths 20-40% of distribution, and so on. Each one has the same number of peptides, and we perform a cross-validation on those lengths. For example, when we test on 0-20% length sequences (i.e., 20% of shortest ones), we use all others for training. As this kind of splitting can introduce heavy class imbalance, we use MCC metric as well suited for imbalanced classification [5], and also report the average positive class percentage (averaged over datasets for AutoPeptideML).

Results are summarized in Tables 26, 27, and 28. Overall, all models exhibit quite similar behavior, with the highest results in the middle 40-60% test bucket, where they can interpolate more from the training data. Results are universally lower for shortest peptides, which contain the least information that the model can use. The performance of molecular fingerprints indicates that they are not particularly negatively affected by peptide size, performing on par with sequence-based baselines.

Table 26. Sequence length split results for AutoPeptideML benchmark.

Model	0-20%	20-40%	40-60%	60-80%	80-100%
ECFP	0.260	0.458	0.482	0.489	0.376
Amino acid counts	0.290	0.409	0.463	0.400	0.355
ESM2	0.262	0.435	0.508	0.527	0.385
Average positive class percentage	52%	51%	47%	51%	48%

Table 27. Sequence length split results for LRGB Peptides-func benchmark.

Model	0-20%	20-40%	40-60%	60-80%	80-100%
ECFP	0.149	0.368	0.418	0.321	0.215
Amino acid counts	0.230	0.419	0.452	0.393	0.268
ESM2	0.099	0.337	0.377	0.293	0.240
Average positive class percentage	13%	17%	18%	17%	17%

Table 28. Sequence length split results for XUAMP benchmark.

Model	0-20%	20-40%	40-60%	60-80%	80-100%
ECFP	0.427	0.577	0.540	0.483	0.427
Amino acid counts	0.285	0.525	0.532	0.496	0.409
ESM2	0.285	0.648	0.675	0.601	0.470
Average positive class percentage	96%	57%	42%	31%	22%

Sequence motif detection

There are tasks that are short-range on sequence level, yet long-range on the molecular graph level. They are challenging for the proposed molecular fingerprints approach, and we provide an example of such as task as an example of peptide therapeutic design task that benefits more from more common baselines. This delineates the applicability domain of the proposed model - if the task requires incorporating order of amino acids, particularly those far from each other in the molecular graph, the sequence-based models have a strong advantage.

The task is recognizing highly charged sequence motifs “KKK” and “RRR” in sequence, which are known to impact peptide-protein binding and are highly relevant to peptide therapeutic design [26, 39, 52]. This is basically checking if there is a substring in the amino acid sequence, and thus is trivial for PLMs like ESM2. It is much harder, but not impossible, for molecular fingerprints, as they ignore order of subgraphs, and thus have very weak learning signal in this task.

We use XUAMP dataset, with the same train and test splits, but replace the original labels with 1 if “KKK” or “RRR” is present in sequence, or 0 otherwise. About 8% of data has positive labels, so we report MCC metric, which works well for imbalanced cases [5]. Molecular fingerprints and amino acid counts use the same models as in the main body, while ESM2-35M is finetuned, in order to show its maximal possible performance. Our goal here is not to achieve any particular performance, but rather show the ability of those methods to incorporate long-range dependencies. Finetuning is kept lightweight and short, with just 2 epochs and learning rate $5 * 10^{-5}$, optimizing BCE loss.

Results are summarized in Table 29. As expected, molecular fingerprints achieve results better than random, but not great. Amino acid counts baseline performs well, while ESM2 gets a near-perfect result.

Table 29. Results on sequence motif detection task.

Model	MCC
ECFP	0.270
Topological Torsion	0.267
RDKit	0.238
Amino acid counts	0.616
ESM2	0.993